Cloning, functional expression and characterization of three *Phanerochaete chrysosporium* endo-1,4-beta-xylanases

Barbara Decelle

A Thesis

In

The Department

Of

Biology

Presented in Partial Fulfillment of the Requirements
for the Degree of Master of Science at Concordia University
Montreal, Quebec, Canada

January 2006

Your file Votre référence
ISBN: 0-494-14221-9
Our file Notre référence
ISBN: 0-494-14221-9

ABSTRACT

Cloning, functional expression and characterization of three *Phanerochaete chrysosporium* endo-1,4-β-xylanases

Barbara Decelle

Three *Phanerochaete chrysosporium* endo-1,4-β-xylanase genes were cloned and expressed in *Aspergillus niger*. Two of these genes, *xynA* and *xynC*, encode family 10 glycoside hydrolases, while the third, *xynB*, codes for a family 11 glycoside hydrolase. All three xylanases possess a type I carbohydrate-binding domain connected to the catalytic domain by a linker region. The three xylanases were purified to homogeneity by weak anion or Avicell column chromatography and subsequently characterized. The XynA, XynB and XynC enzymes have molecular masses of 52, 30 and 50 kDa, respectively. Optimal activity was obtained at pH 4.5 and 70 degrees C with the family 10 xylanases and pH 4.5 and 60 degrees C with the family 11 xylanase. The measured Km when using birchwood xylan as the substrate was 3.71 +/- 0.69 mg/ml for XynA and XynC and was 9.96 +/- 1.45 mg/ml for XynB. Substrate specificity studies and the products released during the degradation of birchwood xylan suggest differences in catalytic properties between the two family 10 xylanases and the family 11 xylanase.

ACKNOWLEDGEMENTS

I wish express my gratitude to my two supervisors Dr Reg Storms and Dr Adrian Tsang not only for accepting me into their crew, but also for their support and their confidence in me. I wish to thank my lab mates, Alain Bataille, Yun Zheng, Enzo Sciffo, Rosa Zito, Nadège Lory, Kimchi Doquang and Xiaoming Li who were there to answer my questions, to help me troubleshooting my experiments or just to have a beer at the McKibbins Pub. Without them my thesis will not have been possible. Thank you too to Sheehab Hossein, Trichia John, Aleks Spurmanis, Peter Ulycznyj, Nathalie Brodeur and Munir Rahim for their theoretical and technical assistance. I also wish to thank Dr Paul Widden for his kindness and the wonderful job he did as my teacher. Thanks to Mathieu Fontaine who taught me the importance of precision, perseverance and good work habits.

I also want to thank my beloved Steeve Lapointe who has been at my side all this time and provided me unwavering stability and moral support. And finally, I wish to thank my whole family for their unwavering encouragement despite the Ocean that lies between us.

CONTENT

LIST OF FIGURES

LIST OF TABLES

ABBREVIATIONS

Å	Ängstrom
Amp	ampicillin
Asp	aspartate
bp	base pair
$CaCl_2$	calcium chloride
CBD	cellulose binding domain
CBH	cellobiohydrolase
cDNA	complementary DNA
CHCA	α-cyano-4-hydroxy-cinnamic acid
CIAP	calf intestinal alkaline phosphatase
CM	complete medium
CMC	carboxymethyl-cellulose
Da	dalton
DDT	1,1,1-trichloro-2,2-bis(4-chlorophenyl)ethane
DEAE	diethylaminoethyl
DNA	Deoxyribonucleic acid
DNSA	3,5-dinitro-salicylic acid
dNTP	deoxynucleoside triphosphate
D. P.	degree of polymerization
EAM	energy-absorbing molecule
EG	endoglucanase

fCBD	fungal cellulose binding domain
g	gram
GFP	green fluorescent protein
G-H	glycosyl hydrolase
Glu	glutamate
GRAS	generally recognized as safe
JGI	Joint Genome Institut
KCl	potassium chloride
LB	Luria-Bertani
M	molar
MALDI-MS	matrix-assisted laser-induced desorption/ionization mass spectrometry
MeGlcA	methylglucuronic acid
MM	minimal media
NMR	nuclear magnetic resonance
opt	optimum
PCR	polymerase chain reaction
PEG	polyethylene glycol
$pNPC_2$	p-nitrophenyl- β-D-cellobioside
pNPG	4-nitrophenyl-β-glucoside
$pNPG_2$	4-nitrophenyl-β-cellobioside
pNPX	4-nitrophenyl-β-xyloside
$pNPX_2$	4-nitrophenyl-β-xylobioside
rpm	revolutions per minute

s	second
SDS-PAGE	sodium dodecylsulfate-polyacrylamide gel electrophoresis
Ser	serine
TFA	trifluoro-acetic acid
Thr	threonine
TLC	thin layer chromatography
TNT	trinitrotoluene
Tris	tris(hydroxymethyl)-aminomethane
Trp	tryptophan
Tyr	tyrosine
U	Unit
USFDA	United States Food and Drug Administration

1. Proposal

Comprising about 42% of Canada's landmass; forests and other wooded land represent an important Canadian resource. Reflecting the importance of this resource, Canada exports over $44 billion in wood, pulp and paper products making it the world's leading exporter of forest products. Generating over 900,000 direct and indirect jobs the forest products sector is one of Canada's largest industrial employers (Natural Resources Canada, http://www.nrcan-rncan.gc.ca/inter/index_e.html).

Within the forestry sector, Canada's paper industry produces 23% of the world's journal paper (Natural Resources Canada, http://www.nrcan-rncan.gc.ca/inter/index_e.html).

Most paper fabrication involves the extraction of plant cellulose fibers from wood chips to produce pulp. A major aim of the extraction process involves bleaching the pulp to remove lignin residues, which contain chromophores that alter the paper color. Pulp is mainly produced using either mechanical pulping or chemical pulping. In the mechanical pulping method, bleaching consists of exposing the pulp to oxygen, whereas chemical pulping involves treating the pulp with chlorine or sulfur compounds. Unfortunately, both of these pulping methods have significant disadvantages. In the case of mechanical bleaching, lignin residues are not removed, resulting in a paper that rapidly turns yellow and that is of relatively poor quality. Concerning chemical pulping, the problem is that it releases pollutants, such as dioxins and chlorinated-lignin compounds into lakes and rivers. It has been demonstrated that such compounds are hazardous and can have environmental repercussions such as altering the sexual behavior of fishes. Concerned by the environmental impact, the Canadian government installed limitations on the amount of chlorinated compounds that can be released by pulping mills. Such measures have led

the pulping industry to adopt biobleaching techniques that include the utilization of xylanases or others hemicellulases. Pre-treatment of the pulp with these enzymes increases bleaching efficiency and therefore reduces the amount of chlorinated compounds released into the environment. Hemicellulases act as biobleaching agents by increasing access to the lignin embedded within the hemicellulose network of xylan and mannan (Bajpai, 2004).

The main goal of my project was to identify fungal xylanases suitable as biobleaching agents for pulp and paper applications. A secondary goal of my project was to test the suitability of *Aspergillus niger* as a host system for the functional expression of heterologous proteins.

2. Introduction

2.1 Plant cell walls

Cell walls are major characteristics of all plants. The role of this complex structure is to protect cells against external stresses. Plant cell walls provide structural and mechanical support, determine and maintain cell shape, and ultimately determine plant structure. The cell wall also prevents expansion due to turgor and protects against pathogens. Cell walls, which contain polymers of cellulose, hemicelluloses and lignin, are the world's major source of fixed carbon. Cellulose is used as a feedstock for the manufacture of cellophane, textiles and, of course, paper. Paper is a product mainly composed of cellulose fibers extracted from woody materials. As interactions between the different compounds forming cell walls are complex, a general description of their structure and the various cell wall components are presented.

2.1.1 General organization of the cell wall in woody plants

The wall of a typical wood cell is composed of multiple layers (Fig.2.1.1). The outermost layer is the middle lamella, which is mainly composed of pectic compounds and proteins. The middle lamella acts as the mortar that binds adjacent cells together. Just below the middle lamella is the primary cell wall. All plant cells have a primary cell wall. The primary cell wall of wood cells is present from cell formation and protects cells against

Figure 2.1.1 Organization of the cell walls of woody plants (Koch P., 1985). The cell wall consists of: P, the primary cell wall; ML, the middle lamella; S1, S2 and S3, the three layers of the secondary cell wall; and, W, the warty layer which is not always present.

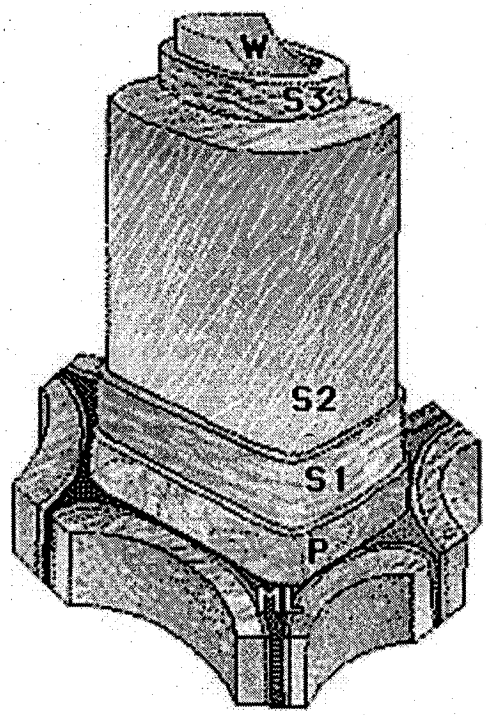
W
S3
S2
S1
P
ML

changes in turgor. The primary cell walls are mainly composed of microfibrils, which are arranges in an "irregular net-like fashion" (http://www.extension.umn.edu/distribution/naturalresources/components/6413ch1.html). The secondary wall is only found in woody cells and is located just beneath the primary wall. Secondary walls form during or after cell expansion and differentiation and are typically composed of three distinct layers, S1, S2 and S3 (Fig. 2.1.1). Major differences between these three layers include the orientation of the microfibrils, their thickness and the cellulose content. The S2 layer is usually much thicker than the S1 and S3 layers. About 30% of the S1 layer (by dry weight) is cellulose, whereas cellulose makes up about 45% of the dry weight of the S2 and S3 layers (Fig. 2.1.1).

2.1.2 Molecular compounds

Cell walls are complex structures known to be very resistant to hydrolysis. Only a selected subset of all non-photosynthetic organisms is able to efficiently digest the various plant cell wall constituents. The resistance of cell wall materials to hydrolysis is due to both the chemical nature of the individual polymers that make up the cell walls and the complex interactions that link the various polymers.

One of the major cell wall components is cellulose. Cellulose is a structural polymer composed of unbranched β-1,4 linked glucose residues. These glucose linkages are very hard to degrade. The cellulose polymers interact via hydrogen bonds and form microfibrils that can adopt both amorphous and crystalline structures depending on the arrangement of the cellulose polymers (Fig. 2.1.2). These microfibrils are themselves arranged in a parallel manner and are sometimes referred to as the 'bricks' of cell walls. In the most popular models, the cellulose microfibrils and higher order cellulose

Figure 2.1.2 Microfibril organization (Purves, 1998). Cellulose chains interact via H-bonds and form microfibrils. Inside microfibrils, cellulose polymers can be arranged in a micelle (crystalline) or an amorphous organization. Microfibrils are held and organized by other polysaccharides such as hemicelluloses that connect them together.

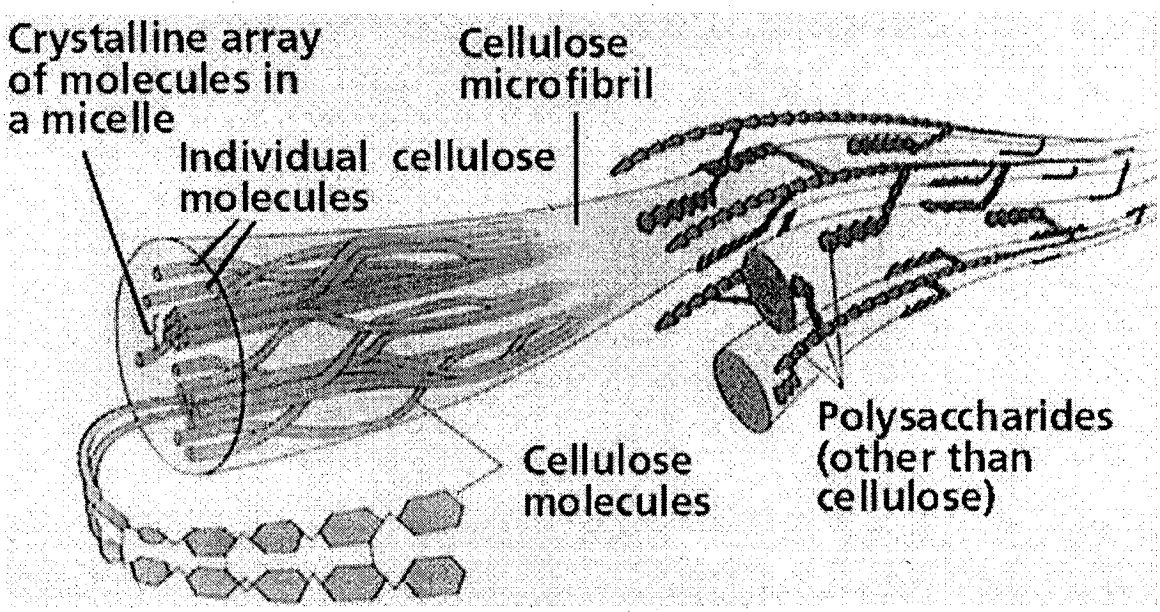
Crystalline array of molecules in a micelle
Individual cellulose molecules
Cellulose microfibril
Cellulose molecules
Polysaccharides (other than cellulose)

structures are coated by hemicellulose, which binds to the cellulose via H-bonding (Rose, 2003) (Fig. 2.1.2 and 2.1.3). The hemicellulose portion of cell walls is often defined as a heterogeneous mixture of polymers with backbones composed of β-1,4-linked pyranosyl residues (Fig. 2.1.4) and includes glucans, xylans and mannans. The galacturonans and rhamnogalacturonans, which contain backbones with α-1,4 or α-1,2 linkages, are called pectins (Fig. 2.1.4). This classification is pertinent because it reflects differences in roles. Pectin microfibrils form a network according to the models presented (Fig. 2.1.3). The pectic network has the properties of a gel and is believed to help organize the cell wall by giving orientation to the other compounds. It was originally proposed that the pectin network was covalently linked to the hemicellulose coated cellulose fibrils. Since only weak interactions have been detected between pectin and the other cell wall carbohydrates, it is now hypothesized that these pectic interactions occur via H-bonds (Rose 2003).

The fourth major macromolecule found in plant cell walls is lignin. Lignin, which is the major noncarbohydrate constituent of wood, is a very complex molecule composed of phenolic residues (Fig. 2.1.5). Lignification is a process that reinforces the rigidity of the cell, and decreases the sensitivity of the cells to biotic and abiotic stress. The complex heterogeneous structure of lignin and difficulties associated with its purification have made it difficult to elucidate its composition, structure and organization within cell walls. Finally, proteins are also important cell wall components. They are usually glycosylated to varying degrees and are often structurally important.

Figure 2.1.3 Models depicting primary cell wall organization. The exact structure of the cell wall is still under investigation. Different models are therefore proposed.

Model A: Hemicellulose polymers coat the cellulose microfibrils. The microfibrils are arranged in a parallel manner. Extensins (cell wall glycoproteins) bind the wall microfibrils together. Pectin cements the hemicellulose coated microfibrils together. (http://cstl-cst.semo.edu/swatzell/BI404/cell%20adhesion/extracellular%20matrix.htm).

Model B: Microfibrils are arranged in parallel planes. Hemicellulose links cellulose fibrils. Pectin forms a network of linkages between individual microfibrils (Rose 2003).

Model A

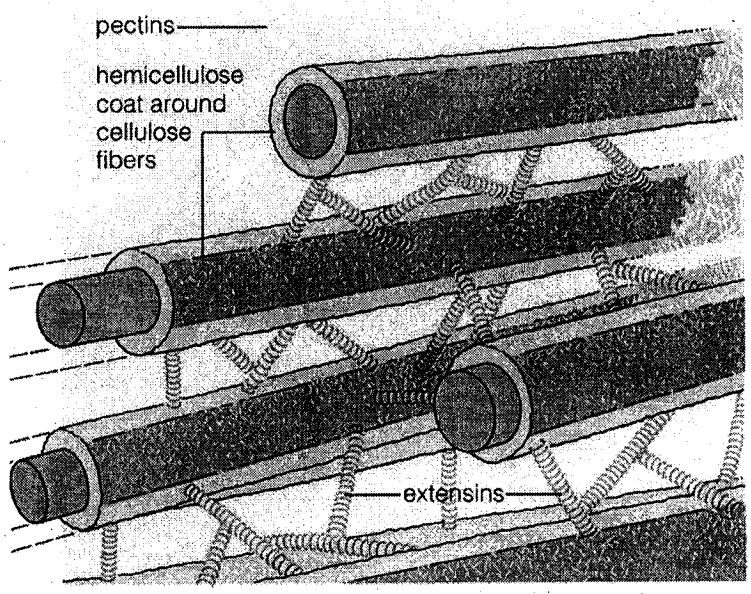

Model B

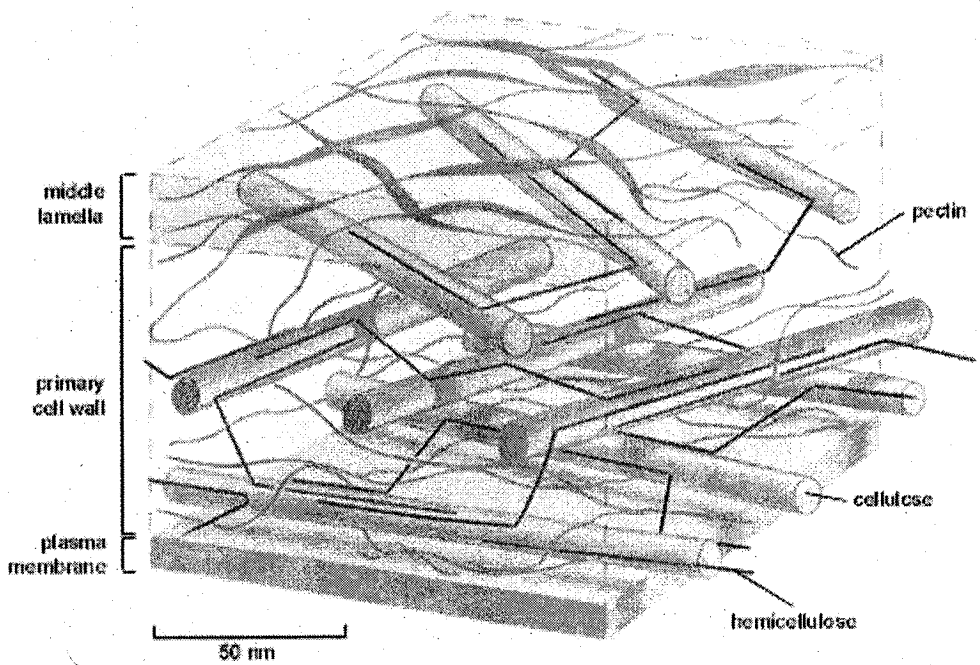

Figure 2.1.4 Structural polysaccharides constituting the cell wall. A. Cellulose. B. Main types of hemicellulose. C. Pectin. D. Legend.

A Cellulose

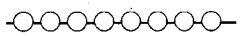

B Hemicellulose

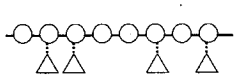

Xyloglucan

Xylan

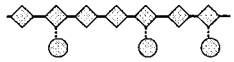

Mannan

C Pectin

Rhamnogalactorunan I

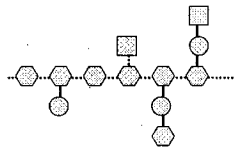

Rhamnogalactorunan II

D Legend

Linkage in β

Glucose

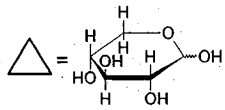

Xylose

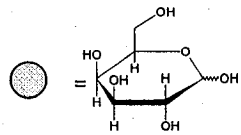

Galactose

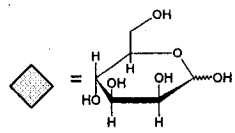

Mannose

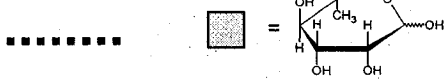

Linkage in α

Rhamnose

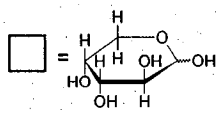

Arabinose

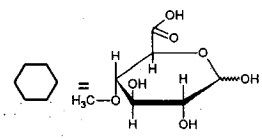

4-O-methyl-Glucuronic Ac.

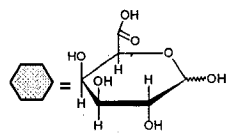

Galacturonic Ac.

Figure 2.1.5 Planar structure of a lignin molecule illustrating the complexity of this compound (Glazer *et al.*, 1995).

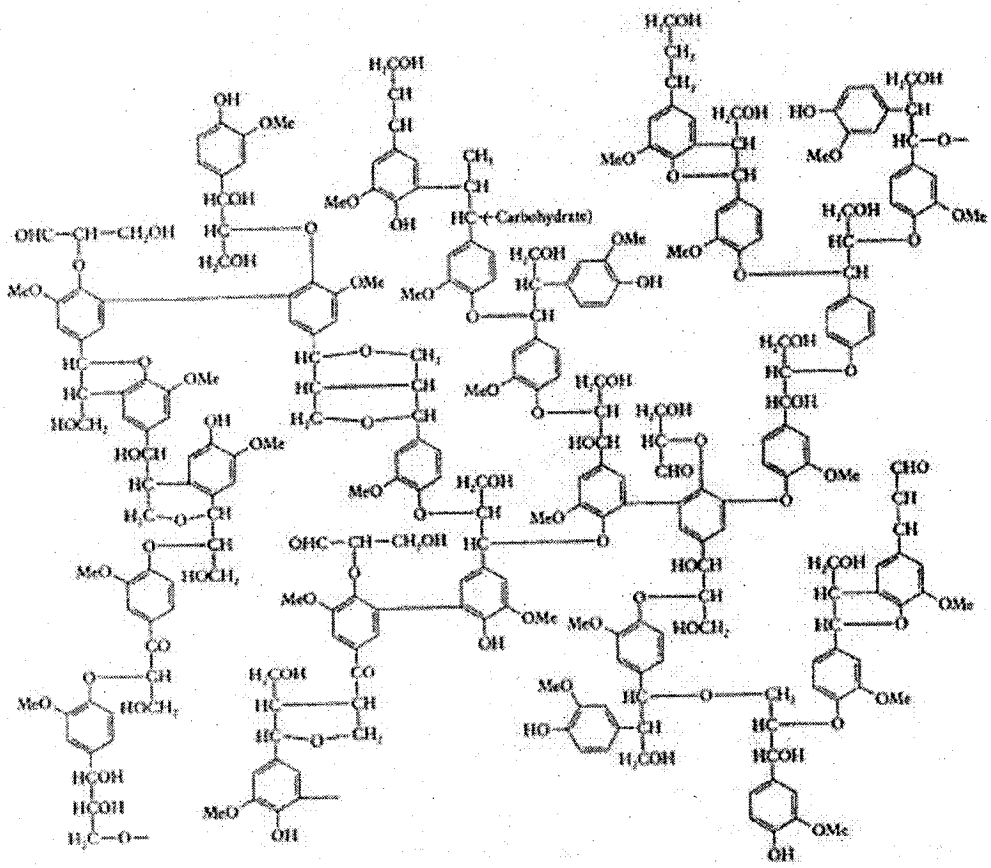

Glazer, A. W., and Nikaido, H. (1995). *Microbial Biotechnology*. New York: W. H. Freeman, p. 340.

Pectic and proteinic compounds are often considered as the cell wall cement, playing critical roles in organizing inter-microfibril interactions within the cell wall and linking the cell wall and plasma membrane.

2.1.3 Differences between the primary and the secondary wall

As mentioned previously, primary and secondary walls fulfill distinct roles; however, their composition also differs. The primary wall contains 1 to 10% of glycoproteins and pectic compounds imparting flexibility to the whole structure and allowing cell wall expansion to accommodate cell growth. In contrast, secondary walls are highly lignified, which makes them strong and rigid. Hemicellulose, common to both primary and secondary cell walls, displays variations in composition: in primary cell walls xyloglucan (Fig. 2.1.4) is predominant and xylans represent only a few percent, whereas in secondary wall structures, xylans and mannans (Fig. 2.1.4) are the most prominent hemicelluloses.

2.1.4 Xylans, occurrence and importance

Xylan is the major hemicellulose found in woody cells. Classically, the type of wood is categorized according the kind of tree, hardwood referring to wood found in leaved-trees and softwood to the wood in conifers. Electron microscopic observations have demonstrated that this classification is relevant and reflects significant structural differences. In addition, analytical studies have shown that the elements composing hardwood and softwood cell walls are also significantly different. In hardwoods, the main hemicellulose is xylan representing 25% to 33% of the dry weight, whereas in softwoods, mannan predominates at about 25% of dry weight, and xylan represents only 5 to 10% of the dry weigh (Jacobs *et al.*, 2001).

2.1.5 Hardwood xylans

O-acetyl-glucuronoxylan (also referred to as O-acetyl-(4-O-methylglucuronan)xylan) is the most common xylan found in hardwood and represents about one quarter to one third of the hardwood total dry weight. It has α-1,2-linked 4-O-methylglucuronic acid (MeGlcA) groups attached to every 10th to 20th xylose residue and 4 to 7 O-acetyl-groups linked via C-2 or C-3 linkages per 10 xylose residues (Fig. 2.1.6). Their degree of polymerization (D.P.) is about 110 to 220 (Teleman *et al.*, 2002). NMR and MALDI-MS studies have found few differences between aspen, birchwood and beechwood xylan. The molecular weight of xylans varies from 8000 for birchwood to 11100 for beechwood. The proportions of MeGlcA are about 5.9, 7 and 9 per 100 xylose residues, for birchwood, beechwood and aspen wood, respectively (Jacobs *et al.*, 2001 & Teleman *et al.*, 2002). Teleman *et al.* (2002) found that the acetylated xylose residues represented 39 % and 42 % of the total for birchwood and beechwood, respectively.

2.1.6 Softwood xylans and non woody xylans

In addition to glucuronic acid and acetyl side groups, softwood xylan also contains α-1,3-linked arabinose residues. Softwood xylans are, therefore, often called arabinoxylan (Fig. 2.1.6). In spruce, pine and larch xylan the arabinose residues are linked to one in every 6 to 11 xylose residues (Jacobs *et al.*, 2001). The proportion of xylose residues substituted with MeGlA is about 14 percent. This ratio is significantly higher than what is observed in hardwood xylans. Furthermore, in contrast to the random distribution observed in hardwoods, the 4-0-methylglucuronic acid residues in softwood xylan are periodically clustered. Xylans found in the bran of the grasses wheat and rice have been found to be arabinoxylans.

Figure 2.1.6 Structure of xylans. A. Diagram depicting the structure of hardwood xylan. **B.** Structure of softwood xylan. **C.** Legend.

A Hardwood xylan

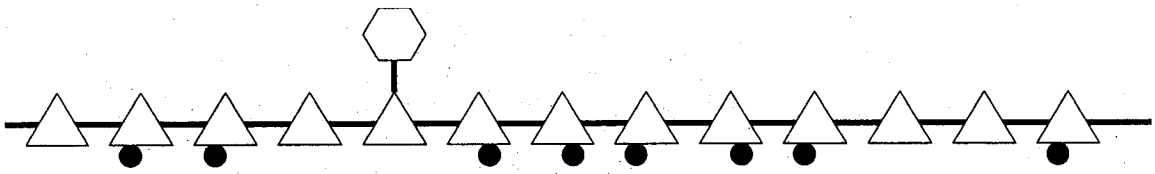

B Softwood Xylan

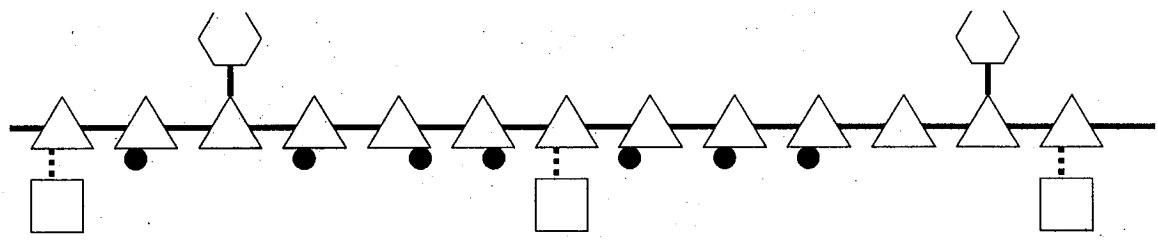

C Legends

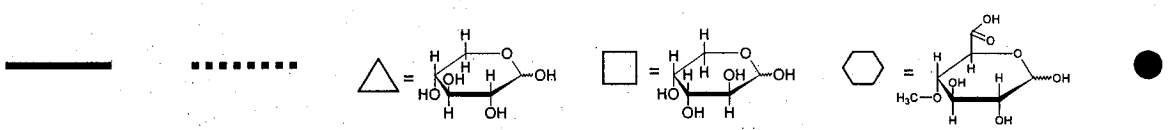

2.2 *Phanerochaete chrysosporium*

Phanerochaete chrysosporium is a resupinate fungus with small fruiting bodies that lives as a saprophyte on the forest floor. *P. chrysosporium* was first isolated in 1964. Discovered under its anamorphic state on wood chips, the fungus was identified as a holobasidiomycetes and then, classified in the *Sporotrichum* genus under the name of *Sporotrichum pruinosum*. Following this discovery, *P. chrysosporium* was re-isolated under other states and received different names such as *S. pulverulatum*, *P. pruinosum* and *Peniophora 'G'*. In 1974 Burdsall and Eslyn proposed the name of *P. chrysosporium* for the teliomorphic state of this fungus. However, the name *C. pruinosum* is still used when referring to the anamorphic state (Young and Akhtar, 1997).

Under its asexual phase, *P. chrysosporium* propagation occurs either via mycelia extension or through the release of conidia. It is possible to induce the formation of basidiospores by acting on temperature and light conditions (Dhawale and Kessler, 1993). Basidiospores of *P. chrysosporium* usually contain two haploid nuclei (Fig. 2.2.1 stage 6d) issuing from meiosis followed by mitosis of the zygote (Fig. 2.2.1 stage 6b and 6c). The resulting spores produce septate and multinucleate mycelia (Dhawale and Kessler, 1993) that can fuse with other compatible mycelia. As in other fungi, karyogamy occurs just before basidia formation. The *P. chrysosporium* mating system is thought to be bipolar heterothallic according to the studies of Thompson and Broda (1987) but this remains unclear due to the order of events occurring during basidia development. Indeed, mitosis can take place before or after the migration of nuclei into basidiospores leading, in the first case, to homokaryotic basidiospores and to the formation of heterokaryotic basidiospores in the second case (Young and Akhtar, 1997). The life cycle of *P. chrysosporium* is presented in Fig. 2.2.1.

Figure 2.2.1 Life cycle of *Phanerochaete chrysosporium* with a bipolar heterothallic mating system (Young and Akhtar, 1997). Released basidiospores (1) form septate mycelia, which contain several haploid nuclei, are able to propagate by hyphal extension or conidia release. When encountering a compatible mycelium (2), hyphal fusion can occur and lead to the formation of a new dikaryotic organism (3). Under certain conditions, the fungus will develop a minuscule fruiting body (4) harboring cystidia (5) and basidia (6). It is only inside the basidia that karyogamy takes place forming a zygote (6a). Zygote development is followed by meiosis (6b), then mitosis and finally the migration of two nuclei into the basidiospores (6d).

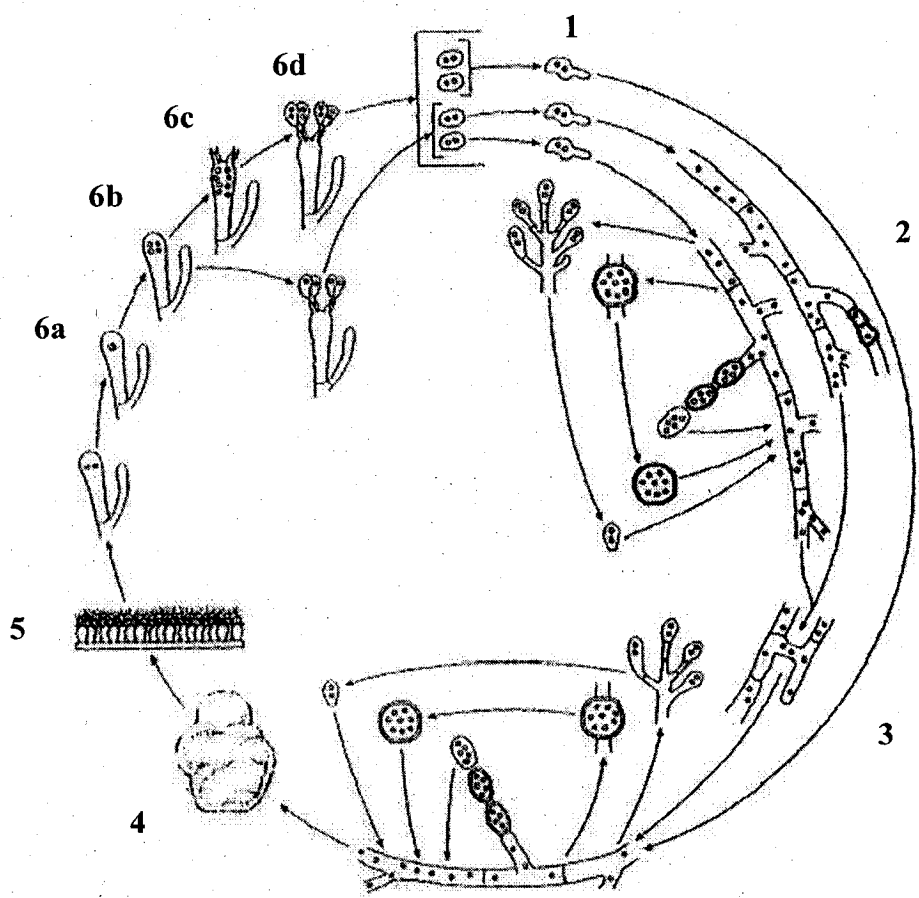
1
2
3
4
5
6a
6b
6c
6d

In its natural habitat, *P. chrysosporium* decays woody materials. Colonized logs take on a white color, which is characteristic of the presence of lignin-free cellulose. Such fungi are called white rot fungi. In contrast, fungi that preferentially use cellulose and degrade the lignin more slowly giving a brownish color to the wood are called brown rot fungi. The ability to degrade lignin is particularly remarkable, since lignin is a complex and non specific substrate composed of aromatic and phenolic compounds. Only white rot fungi have been found capable of efficiently expressing lignin degrading-enzymes such as laccases and lignin peroxidases (Piontek *et al.*, 2001). Interestingly, numerous artificial polymers and pollutant chemicals share properties with lignin compounds. As a consequence, *P. chrysosporium* and other white rot fungi have been obvious candidates when bioremediation processes were seriously investigated. Previous work has shown that *P. chrysosporium* degrades a wide range of chemicals including recalcitrant natural biopolymers such as cellulose and lignin, synthetic polymers like nylon and polyacrylamide, dyes such as cresol red, bromophenol blue and crystal violet, munitions such as TNT, and pesticides such as DDT (Cameron *et al.*, 2000). In addition to the ecological potential of white rot fungi, the biotechnology industries are also interested in the hydrolytic capabilities of these fungi. One potential industrial application involves exploiting the lignolytic activity of *P. chrysosporium* to develop biobleaching agents for the pulp and paper industry, since the quality and the color of paper are negatively impacted by the presence of lignin. For these reasons, *P. chrysosporium* is the model system used for studying the lignin hydrolyzing capabilities of white rot fungi (Cameron *et al.*, 2000). Numerous studies have led to the discovery of a highly conserved lignin degrading gene family (Cameron *et al.*, 2000). Studies have also found that multiple allelic differences can occur between independently obtained clones of the same gene

(Kersten *et al.*, 1995 and Li *et al.*, 1997).The occurrence of highly related gene families and the high degree of allelic difference highlight the difficulties associated with differentiating between these two cases without proper genomic studies. Due to the number of independent strains studied and the complexity of *P. chrysosporium* genetics, it was only recently that a solution to this problem was provided by Stewart *et al.* (2000). They isolated a homokaryon from *P. chrysosporium* strain BKM-F-1767, which was the most studied strain. The resulting homokaryotic strain, RP 78, has the same growth rate and enzyme yields as BKM-F-1767, but possesses only one nuclear type. This is the strain used by the DOE Joint Genome Institute to generate the genome sequence of *P. chrysosporium.*

Availability of the genome sequence of strain RP78 made it an attractive source of new xylanase for pulp bleaching, because only its lignolytic system had been investigated.

2.3 Xylanases (EC 3.2.1.8) and glycoside hydrolases

2.3.1 Xylanase background

Xylanases are expressed by a broad range of organisms, including bacteria, fungi, plants and insects. Xylanases might have different roles depending on the organism that expresses them. In plants, for instance, their role can be related to remodeling the cell wall (McLauchlan *et al.*, 1999) and pollination (Bih *et al.*, 1999); however, in microbial organisms, they often play a central role in xylan degradation.

As xylans are high molecular weight heteropolymers that cannot directly penetrate cell walls, microbial xylanases are secreted into the external environment along with the

others components of the xylanolytic system, which are principally glycoside hydrolases (*e.g.* xylosidases, glucuronidases and arabinofuranosidases) and esterases (*e.g.* acetyl-xylan-esterases and feruloyl esterases). Small xylooligosaccharides released by the combined action of these enzymes enter the cell *via* the action of permeases (Kratzy and Biely, 1980 and Lubomir and Peter, 1998). Once in the cell, xylose is usually integrated into the pentose phosphate cycle by converting xylose into xylitol and furthermore into xylulose, which can be integrated into the hexose monophosphate pathway (Dickinson and Schweizer, 1999).

2.3.2 Classification

Xylanases are endo-enzymes hydrolyzing the β-1,4 linkages of the xylan backbone. Consequently, they are glycoside hydrolases (G-H), a large group of enzymes that cleave glycosidic bonds between two carbohydrates. Until 1991, the main classification for these enzymes was based on enzyme function and substrate specificity. However, as the number of G-Hs increased, it became obvious that a classification system based on sequence homology reflecting the structural features and phylogenic relationships was needed. At the present time, 94 G-H families have been established (Coutinho and Henrissat, 1999). Interestingly, numerous enzymes sharing the same substrate specificity are found in different families suggesting that these enzyme functions have arisen several times during evolution (Henrissat and Davies, 1997). For instance, xylanases principally fall into families 10 and 11. However, a few xylanases belong to family 5 (some bacterial and plant xylanases) and a xylanase belonging to family 8 was recently discovered in an arctic bacterium (Collins *et al.,* 2002). In addition, some families are poly-specific highlighting the fact that, despite the wide substrate diversity of G-Hs, they all have

closely related mechanisms of action. As examples, family 10 G-Hs also include endo-1,3-β-xylanases and cellobiohydrolases, and family 5 G-Hs include mannanases and cellulases. Interestingly, all the G-H family 11 members characterized to date are xylanases.

Most hemicellulosic organisms possess several xylanases. For instance, *Pseudomonas cellulosa* has at least 4 family 10 xylanases (*Xyn10A, Xyn10B, Xyn10C and Xyn10D*) and two xylanases belonging to family 11 (*Xyn11A and Xyn11B*) (Emami *et al.*, 2002). In filamentous fungi, the proportion of xylanases that are family 11 members is reported to be slightly larger than the proportion that are family 10 xylanases (Kulkarni *et al.*, 1999). This is the opposite of what has been reported in bacterial systems. In *Aspergillus niger* all 4 xylanases reported to date are family 11 members, and in *T. reesei*, two of the three known xylanases belong to family 11. In addition to containing numerous xylanase genes, hemicellulolytic organisms can express different xylanase isoforms by alternative splicing, as is the case in *T. reesei* (Lappalainen *et al.*, 2000). The need for individual species to have a diversity of xylanase genes can be explained by the variety of xylans found in nature and the different roles that each xylanase fulfills.

2.3.3 Modular structure

Glycosyl hydrolases can have a structure composed of a single catalytic domain or a modular organization. In some modular G-H there are two catalytic domains while others have a catalytic domain and a non-catalytic module such as a carbohydrate binding domain (CBD), a dockerin domain as is the case for *Clostridium cellulovorans* XynA (Kosugi *et al.*, 2002) or a module for which no function has been assigned (Henrissat and Davies, 2000). The number of modules can vary, as can their organization. XynC from

Clostridium sp. illustrates the modular complexity that can be found in a glycosyl hydrolase. This enzyme possesses a G-H family 10 xylanase domain, a G-H family 43 arabinofuranosidase domain and 6 CBDs belonging to 3 different CBD families (Henrissat and Davies, 2000).

In most cases these functional domains are separated by linkers, which are small poorly conserved threonine, serine, and proline rich regions of 6 to 59 residues (Gilkes *et al.*, 1991). In eukaryotes, these low complexity linker regions are highly O-glycosylated, which is believed to protect them against protease activity (Tomme *et al.*, 1988). It also is believed that these linker regions serve to provide inter-module flexibility (Srisodsuk *et al.*, 1993).

2.3.4 The carbohydrate binding domains

Henrissat *et al.* (2000) also have classified CBDs into families based on their primary amino acid sequence similarity. Their studies identified about 40 families (http://afmb.cnrs-mrs.fr/CAZY/). The only known function of CBDs is carbohydrate binding. Although most CBDs bind cellulose some also bind other polysaccharides. For example, family 2b CBDs interact with both cellulose and xylan, while family 3 CBDs exhibit affinity for chitin.

Interestingly, all the fungal CBDs identified to date belong to CBD family 1. These fungal CBDs interact with amorphous or crystalline cellulose but not soluble cellulose (Srisodsuk *et al.*, 1993).

Type I CBDs are small modules of 35 to 40 amino acid residues arranged in 3 anti-parallel β-strands linked by two or three disulfide bridges (Kraulis *et al.*, 1989, Mattinen *et al.*, 1998) (Fig. 2.3.1). X-ray crystallography has been used to determine the 3-D structure of $CBD_{(CBHI)}$ (Kraulis *et al.*, 1989) and $CBD_{(EGI)}$ (Mattinen *et al.*, 1998), both from *T. reesei*. Both of these CBDs form a wedge-shaped structure composed of one rough hydrophobic surface and one planar surface that exposes hydrophilic and aromatic residues (Fig. 2.3.2) (Kraulis *et al.*, 1989). The planar surface is directly involved in cellulose binding. Several studies aimed at determining the biochemical properties of type I $CBD_{(CBHI)}$ have demonstrated that four amino acid residues, Y7, Y33, Y34 and Q36 are important for carbohydrate binding (Linder *et al.*, 1995) (Fig. 2.3.2). Structural studies found that the distances between the tyrosine residues correspond to the spacing between adjacent glucose residues in a cellulose chain (Mattinen *et al.*, 1997) (Fig. 2.3.2). The fact that three aromatic amino-acids interact with cellulose led researchers to propose a model where Van der Waals forces and aromatic ring polarization are the main forces contributing to binding (Reinikainen *et al.*, 1992, Mattinen *et al.*, 1997 and Carrard *et al.*, 1999). The four amino acids mentioned previously and more particularly Y7, play an important role in determining binding characteristics such as affinity, exchange rates and reversibility. For instance, the single substitution, Y7W in $CBD_{(CBHI)}$, significantly increases affinity (Linder et *al.*,1995), whereas, the inverse substitution in $CBD_{(CBHII)}$, W7Y, decreases affinity. $CBD_{(CBHII)}$-type binding is a more common feature of type I CBDs (Carrard and Linder, 1999). Linder *et al.* (1999) also have constructed pH-dependant CBDs by substituting tyrosines Y7 and Y33 with histidines. The exact nature of the relationship between the CBDs and the catalytic domains is harder to study and remains poorly understood.

Figure 2.3.1 Sequence alignment of *T. reesei* CBDs, $CBD_{(CBHI)}$, $CBD_{(CBHII)}$ and $CBD_{(EGI)}$. The bolded characters indicate residues directly involved in carbohydrate binding, boxes highlight cysteine residues that participate in disulfide bridge formation. Amino acids involved in β-strand structures are underlined by arrows.

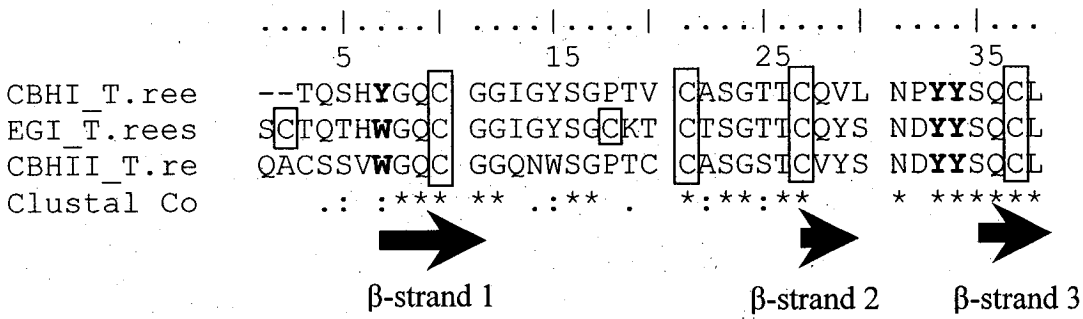
....|....| ....|....| ....|....| ....|...
5 15 25 35
CBHI_T.ree --TQSHYGQC GGIGYSGPTV CASGTTCQVL NPYYSQCL
EGI_T.rees SCTQTHWGQC GGIGYSGCKT CTSGTTCQYS NDYYSQCL
CBHII_T.re QACSSVWGQC GGQNWSGPTC CASGSTCVYS NDYYSQCL
Clustal Co .: :*** ** .:** . *:**:** * ******
β-strand 1
β-strand 2
β-strand 3

Figure 2.3.2 Interaction of CBDs with glucose residues. A. Structure of $CBD_{(CBHI)}$ showing exposed amino acids residues, Y5, Y31 and Y32 on the planar surface (Linder *et al.*, 1995). **B.** Diagram depicting interactions of $CBD_{(CBHI)}$ with glucose residues of cellohexaose (Mattinen *et al.*, 1997). Pyranosyl rings of the cellohexaose are shown in gray whereas amino acid residues are in black.

A

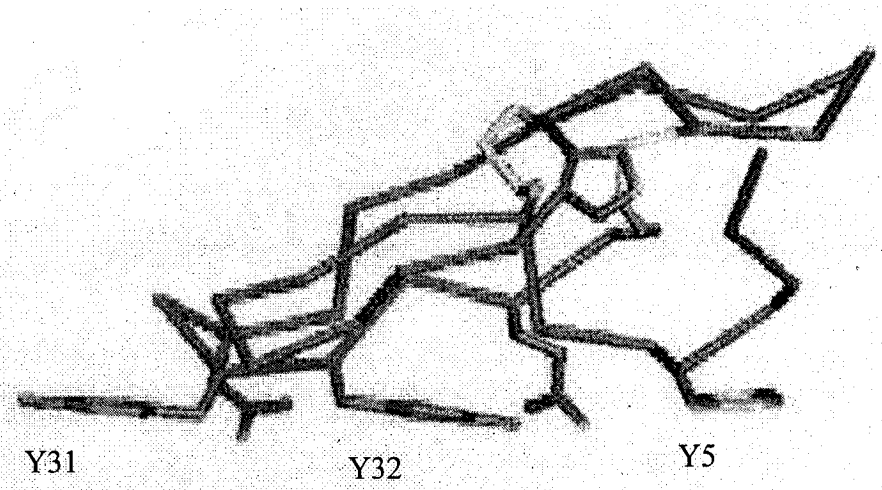

B

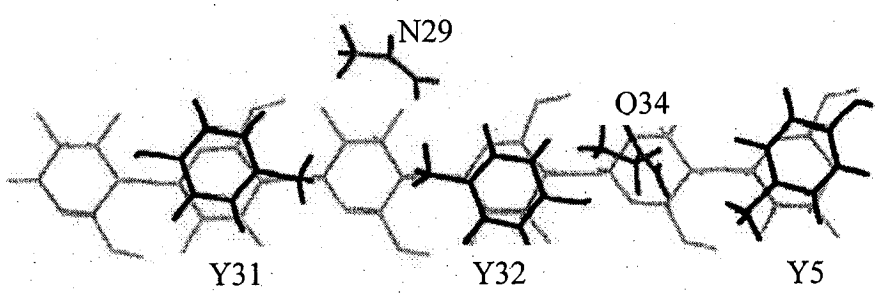

Some studies have demonstrated that removal of the CBD reduces activity of the catalytic module by 50% to 90% (Tomme *et al.*, 1988) when the substrate is insoluble cellulose, but does not have any consequence when soluble cellulose is used. In addition, the catalytic domain seems to enhance CBD affinity toward cellulose (Palonen *et al.*, 1999). However, it is not clear yet if CBDs help break down the cellulose structure or whether they just act by increasing the concentration of enzyme in close proximity of the substrate. The last assumption might explain why CBDs are found in hemicellulases and other cell-wall degrading enzymes, considering the fact that cellulose is intimately associated with these cell wall constituents.

2.3.5 Reactions performed by xylanases

The principal reactions performed by G-Hs are classical acid-base reactions catalyzed by two amino acid residues, one proton donor and one nucleophile, and one molecule of water. Mechanisms, however, can vary and two are well established, the inverting and the retaining mechanisms. 'Inverting' enzymes, or enzymes changing the configuration of the anomeric C, use a single-step mechanism that does not involve formation of an intermediary. The molecule of water, which is activated by the nucleophile, directly attacks the glycosidic linkages (Fig. 2.3.3) (Zechel and Withers, 2001). 'Retaining' enzymes use a two-step mechanism. First, the nucleophile attacks the glycosidic bond, which leads to the formation of an enzyme-substrate complex. The release of the product requires the action of a molecule of water activated by the other residue on the anomeric C (Fig. 2.3.3). All xylanases investigated to date are retaining enzymes that use two glutamate residues as the proton donor and nucleophile.

Figure 2.3.3 Glycoside hydrolase mechanisms (Zechel and Withers, 2001). A. Inverting mechanism of glycoside hydrolases. **B.** Two steps of the retaining mechanism (Zechel and Withers, 2001).

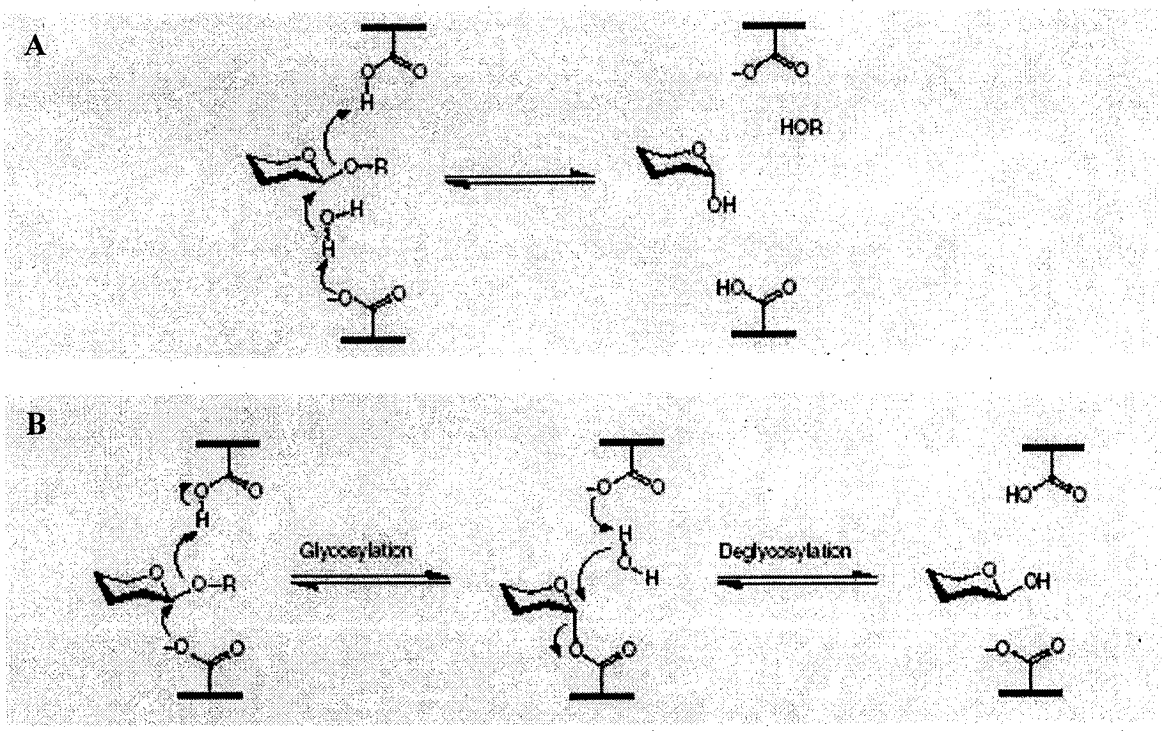
A
HOR
OH
B
Glycosylation
Deglycosylation
OH

Several studies have demonstrated that some xylanases also can perform transglycosylation reactions (Vrsanska *et al.*, 1990, Moreau *et al.*, 1994, Ahrin *et al.*, 1994, Armand *et al.*, 2001). Transglycosylation is the formation of O-glycosidic linkages, which in the case of xylanases are between two xylosyl residues. Although the exact mechanism is not well defined for these transglycosylation reactions, they are known to be slower than the hydrolysis reaction. The transglycosylation products are detectable only under conditions where substrate availability for the principal reaction is low. It has been proposed that these transglycosylation mechanisms could be involved in regulating the xylan-degrading system (Hrmova *et al.*, 1991, Ahrin *et al.*, 1994).

2.3.6 Family 10 xylanases

The family 10 xylanases, which are also called high molecular weight xylanases in comparison to family 11 xylanases, have a catalytic domain of about 35 kDa. Family 10 xylanases are thought to bind xylan and other substrates by numerous hydrophobic interactions and H-bonds. Analysis of the products generated by several family 10 xylanases indicated that when the substrate is hardwood xylan, the largest non-degradable oligosaccharide is aldotetrauronic acid (MeGlcAXyl3) (Biely *et al.*, 1997 and Christakopoulos *et al.*, 2003). The NMR-defined structure of aldotetrauronic (Fig. 2.3.4), suggests that family 10 xylanase can hydrolyze linkage next to glucuronic acid substituted xylose residues (Biely *et al.*, 1997). This hypothesis is in agreement with recent work performed by Pell *et al.* (2004) on a *Cellvibrio mixtus* xylanase. Their analyses showed that uronic acid binds to the +1 subsite *via* hydrogen bonds and hydrophobic interactions, thereby influencing cleavage positions.

Figure 2.3.4 Structure of uronic acids. A. Structure of aldotetrauronic acid. **B.** Structure of aldopentauronic acid.

A

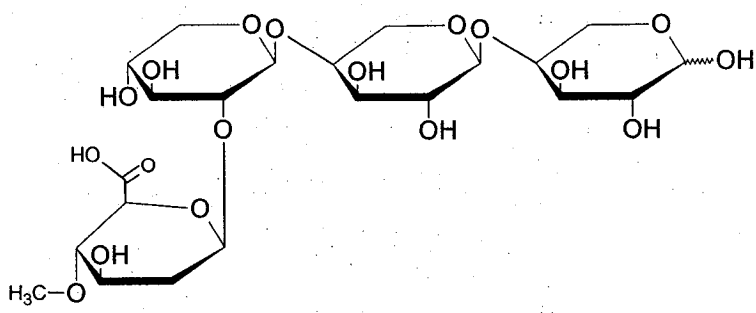

B

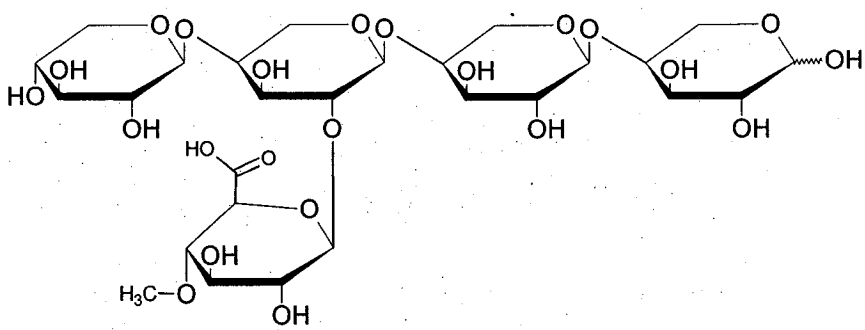

The presence of arabinose residues in softwood xylan has made it more difficult to resolve its degradation by family 10 xylanases. However, results suggest that enzyme cleavage may be dependent on the position of the arabinose substituent. Biely *et al.* (1997) suggest that L-arabinose at position 2 may actually be more favorable than substitution at position 3.

In addition to their principal xylanolytic activity, most family 10 xylanases exhibit activity toward short hexo-oligosaccharides such as 4-nitrophenyl-β-glucoside (pNPG) and 4-nitrophenyl-β-cellobioside ($pNPG_2$) and pento-oligosaccharides such as 4-nitrophenyl-β-xyloside (pNPX) and 4-nitrophenyl-β-xylobioside ($pNPX_2$). This has led researchers to consider that they also have an exo-activity. Despite the similar linkages between the xylose residues in xylan and the glucose residues in cellulose, family 10 xylanases display very poor abilities to degrade cellulose. This may result because the planar structure of cellulose is a less favorable substrate than is the threefold left-handed helical structure of xylose oligosaccharides (Fig. 2.3.5) (Leggio *et al.*, 2000). Crystallography performed on numerous family 10 microbial xylanases (Derewenda *et al.*, 1994, Harris *et al.*, 1994, White *et al.*, 1994, Dominguez *et al.*, 1995, Schmidt *et al.*, 1998, Leggio *et al.*, 2000) has demonstrated that their structures are well conserved. The enzyme cores are composed of a β-barrel bearing the two catalytic residues on strands 4 and 7 separated by about 5.5 Å (Schmidt *et al.*, 1998).The β-barrel is surrounded by α-helixes that form a structure called $(\alpha/\beta)_8$ or TIM-barrel (Schmidt *et al.*, 1998) (Fig. 2.3.6). Surface representations of *Penicillium simplicissium* and *Cellulomonas fimi* (Fig. 2.3.7) xylanases show a wide cleft crossing the top of the enzymes where the catalytic sites and binding subsites are located.

Figure 2.3.5 Diagram depicting cellulose and β-1,4 linked xyloses structure (Leggio *et al.*, 2000). Hydrogen bonding due to the presence of a hydroxyl group on C6, gives a planar structure to cellulose molecules, whereas the xylan backbone adopts a helical structure.

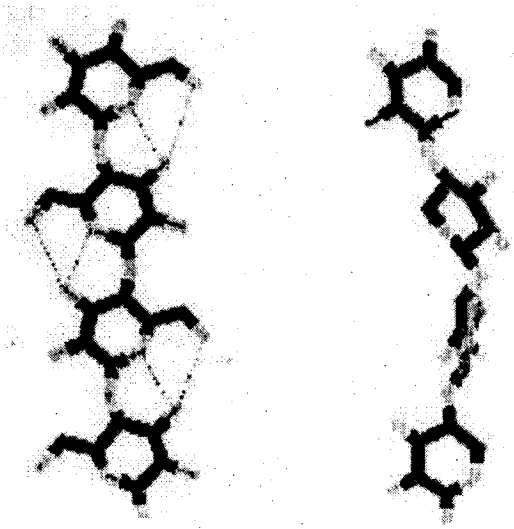

Cellulose Xylan

Figure 2.3.6 TIM-Barrel structure of family 10 xylanase (Schmidt *et al.*, 1998). Diagram depicting the ribbon structure of family 10 XynC from *P. simplissium*. The enzyme core, constituted of one β-barrel, contains the two glutamates of the active site. α-helixes surround the enzyme catalytic site.

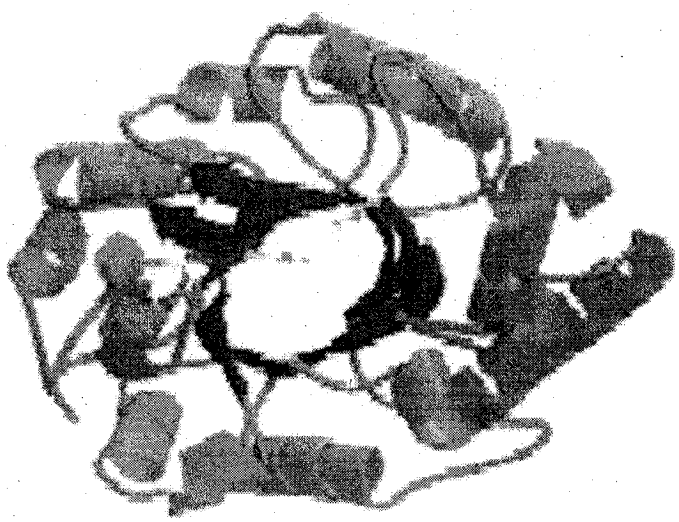

Figure 2.3.7 Surface representations of *P. simplissium* (A) and *C. fimi* (B) xylanases (Schmidt *et al.*, 1998). Wide clefts with active site residues inside are visible, crossing the middle of the enzyme.

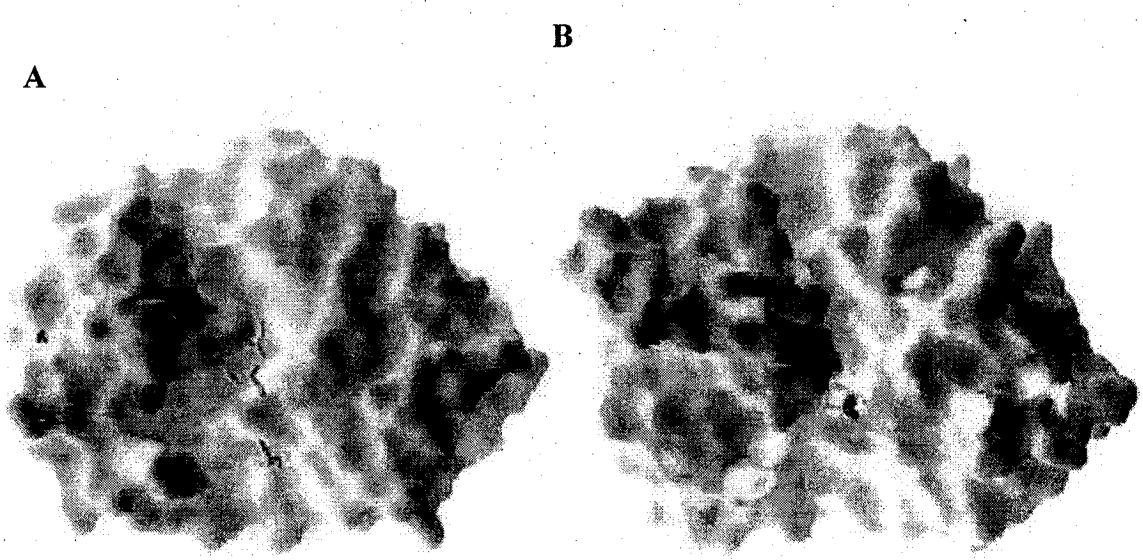
A
B

If general the 3-D structure and the catalytic sites are well conserved amongst family 10 xylanases, the case of the binding site is more complex. Structural studies have shown that the topology of binding clefts is not conserved (Charnock *et al.*, 1998 and Schmidt *et al.*, 1998) and that the number of defined subsites varies from one enzyme to the other. For instance, XynA from *C. fimi* possesses three glycone subsites (-) and two aglycone subsites (+), which bind the reducing end of the substrate. *Pseudomonas cellulosa* XynA has three glycone and four aglycone subsites and for *P. fluorescens* XYLA there are two or three glycone subsites and four aglycone subsites (Charnock *et al.*, 1998 and Leggio *et al.*, 2000). Numerous studies indicated that subsites -2, -1 and +1 are the most important ones for the binding and hydrolysis of small substrates (Charnock *et al.*, 1998, Andrews *et al.*, 2000, Ducros *et al.*, 2000). Interestingly these residues are highly conserved (Leggio *et al.*, 2000); however, structural analyses have shown that they adopt different conformations from one enzyme to another allowing different tolerance to small substrates. This may explain the significant variations in catalytic efficiency toward small substrates (kcat/Km) that exist among family 10 members (Table 2.3.1). Other studies have assigned putative roles for these subsites in a *P. fluorescens* xylanase. The work of Charnock *et al.* (1998) suggests binding to the -2 and +1 subsites ensures that small substrates are positioned at the -1 and +1 subsites. The results of Leggio *et al.* (2000) indicate that interaction of the -1 subsite with a xylosyl residue distorts the substrate thereby facilitating catalysis.

Table 2.3.1. Variation of catalytic efficiency (kcat/Km) of three family 10 xylanases toward small aryl-substrates (Ducros *et al.*, 2000).

	k_{cat}/K_M ($s^{-1}.mM^{-1}$)		
Substrates	Xyl10A (*S. lividans*)	Xyl10A (*P. cellulose*)	Cex (*C. fimi*)
pNPG	6.9×10^{-4}	Not Detectable	6.0×10^{-3}
$pNPG_2$	0.071	0.052	13.8
pNPX	8.1×10^{-4}	4.8×10^{-4}	0.09
$pNPX_2$	50.7	151.6	1952

2.3.7 Family 11 xylanases

Family 11 xylanases, sometimes called the true xylanases, have catalytic domains that are about 20 kDa, which is smaller than those found in family 10 xylanases. Like family 10 xylanases, they use a retaining mechanism to hydrolyze O-glycosidic linkages and are capable of performing transglycosylation. Nonetheless, family 10 and family 11 xylanases exhibit numerous differences in catalytic properties. The first major report outlining these differences was published by Biely *et al.* (1997). Their study showed that both types of xylanase do not release the same product from hardwood and softwood hydrolysis. As mentioned previously, family 10 members released aldotetrauronic acid, whereas family 11 xylanases produced aldopentauronic acid (Fig. 2.3.4) as the shortest acidic fragment. Furthermore the methyl-glucuronic acid substituent in the aldopentauronic acid is linked to the penultimate non-reducing end xylosyl residue (Fig. 2.3.4). These and other results (Vardakou *et al.* 2003 and Christakopoulos *et al.* 2003), suggest that family 11 xylanases are more affected by the presence of substituents and are not able to cleave linkages between substituted and unsubstituted xylosyl residues. Additional results show that hydrolysis of xylooligosaccharides by family 11 xylanases requires the presence of at least three unsubstituted xylosyl residues (Biely *et al.*, 1997, Christakopoulos *et al.*, 2003 and Vardakou *et al.*, 2003).

Activity of family 11 xylanases toward small aryl substrates has been poorly investigated at the present time. Biely *et al.* (1997) have tested four family 11 xylanases without detecting significant activity. However, one study reported that a *Bacillus circulans* xylanase exhibits activity toward $pNPX_2$ (Joshi *et al.*, 2000) with a catalytic efficiency of 35 $s^{-1}.mM^{-1}$.

At the present time, the most studied catalytic properties are pH optimum and temperature stability, which are both important for industrial applications. Family 11 xylanases often are classified as acidic and alkaline xylanases based on their pH optima. Structural studies have been performed on numerous family 11 microbial xylanases, such as *B. circulans* (Wakarchuk *et al.*, 1994), *T. reesei* (Torronen *et al.*, 1994 and Torronen and Rouvinen, 1995), *A. niger* (Krengel and Dijkstra, 1996) and *Aspergillus kawachii* (Fushinobu *et al.*,1998). Crystallographic analyses showed that they all share a 'unique' structure composed of one alpha-helix and two-twisted beta-sheets, A and B (Fig. 2.3.8). This structure, which is sometimes compared to a 'right hand' (Torronen and Rouvinen, 1995), forms a wide cleft (Fig. 2.3.8) where the active site residues and binding subsites are located. Within this cleft, also called the pocket, are numerous exposed Trp, Tyr and Phe residues that surround the catalytic site. Site-directed mutagenesis studies performed on *A. niger* (Tahir *et al.* 2002) and *Streptomyces* sp. S38 (de Lemos Esteves *et al.* 2004) xylanases have clearly demonstrated that these residues are directly involved in xylan binding.

Studies performed by Fushinobu *et al.* (1998) with the acidic XynC from *A. kawachii* demonstrated that Asp37 (D37) was an important determinant of its pH optimum. Mutating the XynC D37 residue, located in close proximity of catalytic residue Glu170, to an asparagine (N) residue, increased the optimum pH from 2 to 5. Sequence alignments of 82 family 11 members supported the notion that the D residue was highly conserved amongst all except one of the acidic xylanases (Sapag *et al.*, 2002), acidic being defined as exhibiting a $pH_{opt} < 5$ (Sapag *et al.*, 2002).

Figure 2.3.8 Xylanase structure of family 11 members. A. Ribbon structure of *T. reesei* XYNI, β-strands are named according to their belonging to β-sheet A or β-sheet B. **B.** Analogy with the right hand model (taken from Torronen and Rouvinen, 1995)

A

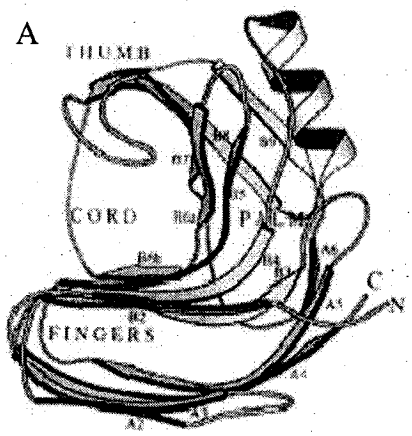

B

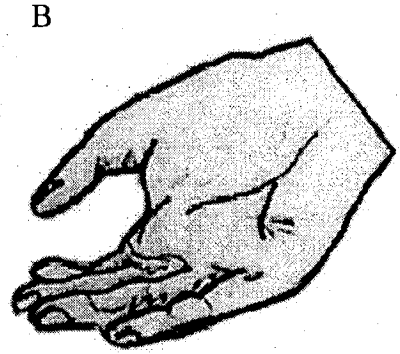

In alkaline xylanase, the D residue is replaced by an N, which cannot stabilize the transition state of the enzyme substrate complex via formation of a hydrogen bond between the catalytic D residue and the acidic E residues (Fushinobi *et al.*, 1998 and Joshi *et al.*, 2000).

One other region of family 11 xylanases, the Ser/Thr region (Fig. 2.3.8), may affect their $pH_{opt.}$. By changing four or five residues belonging to the XYNII Ser/Thr region, Turunen *et al.* (2002), increased the XYNII $pH_{opt.}$ by 1.4 units. Unfortunately, such mutations decrease thermostability in the absence of substrate.

Temperature stability also has been investigated; however, key factors have not yet been successfully identified. One common hypothesis was that disulfide bridges might increase stability; but sequence alignments indicated that their presence does not contribute to thermostability. Seven thermostable xylanases were investigated and only three formed disulfide bonds. Furthermore, disulfides bonds are found in enzymes exhibiting temperature optima of only 50°C (Sapag *et al.*, 2002). Finally, as no characteristic features have been found to be shared by thermostable family 11 xylanases, it has been concluded that their thermostability is not determined by a unique factor.

2.4 Expression system

The xylanases described in this study were expressed in the filamentous fungus *A. niger*. This fungus is a convenient host for protein expression, because it has been extensively studied, it is Generally Recognized As Safe (GRAS) by the United States Food and Drug Administration (USFDA) and it already has been used in our laboratory as a host for protein expression. *A. niger* is quite easy to manipulate, it can grow in inexpensive media at pHs ranging from 1.5 to 9.8 and can be cultured at temperatures varying from 17°C to

42°C. Also important, *A. niger* and *P. chrysosporium* use the same genetic code, and *A. niger* has been found to be able to secrete high levels of homologous proteins, sometimes reaching $30g.l^{-1}$ (Punt *et al.*, 2002). Such high levels of expression are rarely reached using other expression systems, including yeast strains. In addition, yeasts strains such as *Saccharomyces spp.* and *Pichia spp.* produce hyper mannosylations that can alter enzyme activity (Punt *et al.*, 2002).

However, previous studies found that high secretion levels are harder to reach when using *A. niger* to express foreign proteins. Several filamentous fungi, including *A. niger,* express high amounts of proteases and research using the Green Fluorescence Protein (GFP) (Gordon *et al.*, 2000) demonstrated that proteolysis can be a factor that limits the expression of heterologous proteins.

To facilitate protein expression in *A. niger*, genes were cloned into an autonomously replicating multicopy vector (Storms *et al.*, 2005). This plasmid (Fig. 2.4.1) was assembled from several cassettes that included; a pUC derived cassette that confers ampicillin resistance and supports autonomous replication in *E. coli*; the AMA1 element that allows autonomous replication of the plasmid in the fungus, a selection marker (pyrG), and finally unique *Nhe*I and *Fse*I cloning sites within an *A. niger* expression cassette that includes the glucoamylase promoter region (GlaPr) and transcription terminator (GlaTer). The *A. niger* GlaPr is a strong promoter that has been extensively studied and used for its ability to express proteins at high levels (Carrez *et al.*, 1990, Fowler *et al.*, 1990, Hata *et al.*, 1992, Jeenes *et al.*, 1993, Verdoes *et al.*, 1993, Withers *et al.*, 1998, Santerre Henriksen *et al.* 1999). The TATAA element and the transcription initiation sites are located at -111 bp and –83 bp relative to the translation start codon (Nunberg *et al.*, 1984). In addition, GlaP is highly regulated. Maltose or glucose induces

Figure 2.4.1 The ANEp2 vector. Ap/pUC18 region, derived from plasmid pUC18, harbors the ampicillin resistance gene (Ap) and an origin of replication for selection and autonomous replication in *E. coli*; AMA1 region, supports autonomous replication in *A. niger*; pyrG gene, marker for selection of transformants in *pyrG⁻ A. niger* strains; GlaPr-LacA- GlaTt, expression cassette region with the coding region of the *A. niger* LacA (β-galactosidase) flanked by the glucoamylase gene (*GlaA*) transcription and translation control sequences (GlaPr) and the transcription termination and polyadenylation control sequences (GlaTt). Gene coding regions can be expressed in *A. niger* following insertion into the ANEp2 backbone, prepared by *Fse*I and *Nhe*I digestion.

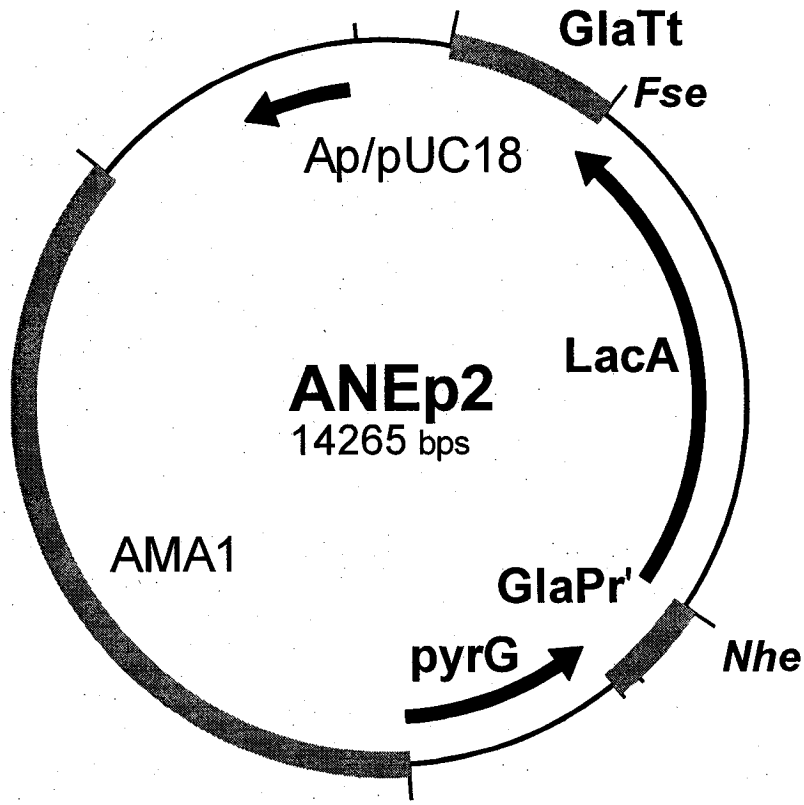
GlaTt
Fse
Ap/pUC18
LacA
ANEp2
14265 bps
AMA1
GlaPr'
pyrG
Nhe

its expression, whereas it is repressed when xylose is used as the sole carbon source.

3. Materials and Methods

3.1 Predictions and computer analysis

The Blast algorithm was used to find the sequences for three putative xylanase genes in the genome sequence of *P. chrysosporium* (Joint Genome Institute http://www.jgi.doe.gov/programs/whiterot/whiterot_mainpage.html). The *A. niger* endo-1,4-xylanase (accession number: AF490982) gene sequence was used to find *xynB* whereas *xynA* and *xynC* were found by searching with the *Aspergillus oryzae* endo-1,4-xylanase F3 entry (accession number: JC7813). The signal peptide of each xylanase was identified using the SignalP Server (http://www.cbs.dtu.dk/services/SignalP/) (Nielsen *et al.*, 1997), and the determination of conserved protein domains was performed using the NCBI CDART (Conserved Domain Architecture Retrieval Tool) (http://www.ncbi.nlm.nih.gov/Structure/lexington/lexington.cgi?cmd=rpsand) and EXPAZY ScanProsite (http://us.expasy.org/tools/scanprosite/) websites (Appel *et al.*,1994). The pI of the proteins and potential N-glycosylation sites were identified using the PepTool© software. Potential O-glycosylation sites were identified using the YinOyang site (http://www.cbs.dtu.dk/services/YinOYang). Finally the predicted 3-D structures were generated using the Swiss-model program (http://us.expasy.org/sw3d/) (Peitsch, 1995; Guex *et al.*, 1997; Schwede *et al.*, 2003).

3.2 Strains and plasmid

P. chrysosporium strain RP78, provided by the United States Department of Agriculture Forest Product Laboratory, was used as the source of genomic DNA for the amplification of endo-1,4-β-D-xylanase genes. *A. niger* strain N593 (cspA1, pyrG6), provided by C. J.

Bos, was used as the host for heterologous protein expression. *E. coli* strain DH5 α was used as the host for the construction and propagation of recombinant plasmids.

The autonomously replicating plasmid ANEp2 (Storms *et al.*, 2005) was employed as the expression vector for the production of xylanases of *P. chrysosporium* in *A. niger*.

3.3 Media and culture conditions

E. coli cultures were incubated for 14-16 hours at 37°C in LB medium supplemented with 100 mg/L of ampicillin. The LB medium consisted of 1% (w/v) tryptone, 1% (w/v) of yeast extract, and 0.5% (w/v) of NaCl. *A. niger* cultures were grown in either complete medium (CM) or minimal medium (MM) (Käfer, 1977) with 15% (w/v) maltose, 15% (w/v) glucose or 5% xylose as the carbon source. Liquid cultures were inoculated in two ways: one used conidia to inoculate cultures at a concentration of 10^6 conidia/mL of medium and the other used a piece of agar, which contained mycelia of the *A. niger* strain of interest. Liquid cultures were maintained at 150 rpm in a rotary shaker. Both solid support and liquid cultures of *A. niger* were grown at 30°C.

3.4 Cloning

3.4.1 Gene amplification

Three pairs of primers, complementary to the beginning and the end of the coding sequence of three *P. chrysosporium* xylanase genes were used to amplify genomic DNA. To facilitate cloning the PCR products into expression vector ANEp2, each forward primer contained a *Nhe*I restriction site and each of the reverse primers a *Fse*I restriction site (*xynA*: forward: 5'-CCTAGCTAGCATCATGAAGCTCTCAGCCTCCTTCG-3' reverse 5'-TCTTAGGCCGGCCCTAATTGCCGAAGCCAATAGCG-3', *xynB* forward: 5'-

CCTAGCTAGCATCATGGTCAGCTTCAACTCCCTCC-3', reverse: 5'-TCTTAGGCCGGCCTTAGAGGCACTGGGAGTACCAG-3', *xynC*: forward: 5'-CCTAGCTAGCATCATGTTCAAGTTCTCCGCGTCC-3', reverse 5'-TCTTAGGCCGGCCTCATGCGCTGAAGCCAGCG-3'). Gene amplifications were performed in 50 µL reaction volumes using 2.5 units of Pfu polymerase and 300 ng of *P. chrysosporium* genomic DNA. The final concentration of primers, dNTPs and $MgSO_4$ were 0.5 µM, 0.4 mM and 1.5 mM, respectively. The PCR reactions of 25 to 35 cycles were carried out at annealing, extension and denaturation temperatures of 52°C, 72°C and 94°C. The resulting PCR products were purified by phenol/chloroform extraction and precipitated using ammonium acetate (0.2 volume of 3M) and cold ethanol (2.5 volumes of 99% ethanol). Finally, the PCR products were prepared for insertion into the expression vector by digestion with restriction endonucleases *Fse*I and *Nhe*I. All DNA processing enzymes were obtained from Fermentas or New England Biolabs

3.4.2 Backbone preparation

The ANEp2 backbone was prepared by digestion using *Fse*I *and Nhe*I. Digestion products were incubated for 15 minutes at 37°C and for 45 minutes at 55°C with CIAP (provided by New-England Biolabs) in order to remove the 5'-phosphates at each end of the vector. Following a phenol/chloroform extraction, the backbones were ready for ligation.

3.4.3 Plasmids constructions and *E. coli* transformation

Inserts and ANEp2 backbone were ligated for 4 hours at 16°C and reaction products were used to transform *E. coli* competent cells following the basic heat-shock protocol for

$CaCl_2$ treated cells (Hanahan, 1983). Transformed DH5α cells were selected on LB + Amp plates and three independent plasmid constructs harboring each xylanase gene were identified by restriction endonuclease analysis. The plasmid constructs were designated as ANEp2-xynA-1, ANEp2-xynA-2, ANEp2-xynA-3, ANEp2-xynB-1, ANEp2-xynB-2, ANEp2-xynB-3, ANEp2-xynC-1, ANEp2-xynC-2 and ANEp2-xynC-3.

3.4.4. *A. niger* protoplasting and transformation

A. niger protoplasts were prepared as described previously (Debets and Bos, 1986). A flask of liquid CM medium was inoculated and incubated as described in section 3.3. After 14 hours, mycelia were filtered through Miracloth™, weighed, and transferred into lytic buffer (50 mM maleic acid and 0.6 M ammonium sulphate, pH 5.5) containing mutanase (10mg/mL). After 1 to 2 hours of incubation at 30°C and 150 rpm, protoplasts were centrifuged (2500 × g for 10 minutes) and washed three times; once with 0.7 M KCl solution and twice with the S/C solution (1 M sorbitol and 50 mM $CaCl_2$). Finally, in preparation for transformation, protoplasts were suspended in S/C solution at a concentration of 1×10^8 protoplasts/mL.

Two hundred µL of the protoplast suspension were mixed with 1 to 10 µg of plasmid DNA and 50 µL of PEG solution (25% (w/v) polyethyleneglycol 8000, 50 mM $CaCl_2$ and 10 mM Tris-HCl pH 7.5) and incubated for 20 minutes on ice.

This first incubation was followed by the addition of 200 µL of PEG solution and a second incubation of 5 minutes. Four hundred µL of S/C then were added. Protoplasts were centrifuged for 10 minutes at 2500 × g and the pellets were resuspended in 200 µL of S/C buffer. Transformants were plated on MM agar plates containing KCl (44.7 $g.L^{-1}$) using an agar overlayer.

3.5 Production and purification of enzymes

The cloned xylanase genes were expressed in *A. niger* strain N593. After growth in liquid medium for 2 days, cultures were filtered through miracloth^{TM} to remove the mycelia and the xylanases were purified from the culture filtrate as follows: the proteins were concentrated and partially purified by ammonium sulfate precipitation (60% for XynA and XynC and 80% for XynB). The precipitated proteins then were resuspended in either 10 mL of sodium acetate (50 mM, pH 6), or with the buffer required for the next purification step – i.e., overnight dialysis at 4°C. For XynA and XynB, the dialyzed samples were purified by affinity chromatography using Avicell as the matrix. Proteins were loaded onto the affinity column, previously equilibrated with Tris-HCl (20 mM, pH 7.5) and NaCl (4 M). After loading the proteins, the column was washed with 10 column volumes using a gradient of 4 to 0 M NaCl. Bound xylanases were eluted from the column using 5 column volumes of 100% ethylene glycol (Carrard *et al.* 2000). Fractions containing the peak of xylanase activity were pooled and dialyzed against sodium acetate (50 mM, pH 6).

XynC was purified using a different method. After 60% ammonium sulfate precipitation, the precipitate was dissolved into Tris-HCl (20 mM, pH 8) buffer. The redissolved precipitate was then heated at 57°C for 30 minutes followed by centrifugation at 10000 ×g for 30 min at 4°C. The supernatant was loaded onto a weak anion exchange column (DEAE), previously equilibrated with Tris-HCl (20 mM, pH 8). Proteins were eluted from the column with a linear gradient of 0 to 0.4 M NaCl at a flow rate of 0.75 mL per minute. Fractions containing the highest xylanase activity were pooled and dialyzed against sodium acetate (50 mM, pH 6).

Electrophoresis was performed on 10% SDS-PAGE gels. Proteins were visualized either by Coomassie blue R250 staining or silver staining (Biorad).

3.6 Mass spectrometry

Proteins bands were excised from a SDS-PAGE gel and washed twice in ammonium bicarbonate (0.1M, pH 8) for 10 min. Gel pieces then were incubated in a solution of 50% acetonitrile/0.1 M of ammonium bicarbonate (pH 8) and shaken gently at room temperature. After 1 hour of incubation, the buffer was removed and protein bands cut into smaller pieces. The remaining SDS contained in the gel was removed by a final incubation of 15 minutes in 100% acetonitrile. Gel fragments were dried using a speed vacuum and incubated overnight at 37°C in a water bath with a solution of ammonium bicarbonate (0.25M pH 8) containing trypsin.

For mass spectroscopy, one µL of sample was loaded onto the chip and covered with 0.5 µL of EAM solution (10% v/v acetonitrile, 0.5% of TFA and 20% of saturated CHCA α-cyano-4-hydroxy-cinnamic acid saturated solution).

3.7 Enzyme assays

Xylanase activity was assayed by measuring the production of reducing sugar ends from birchwood xylan (Sigma) with DNSA (3,5-dinitro-salicylique acid) reagent (1% w/v DNSA from Sigma, 30% w/v Rochelle Salt and 0.4N NaOH). Fifty µL of crude or purified xylanases in sodium acetate (50 mM, pH 6) were incubated with 50 µL of 1% (w/v) birchwood xylan (Sigma) in the same buffer at 60°C. After 10 min., 50 µL of DNSA reagent was added and the samples were boiled for 10 min. Reducing sugar production was determined by measuring the absorbance at 540 nm (*Sengtupta et al.*

2000) and using a standard curve generated with D-xylose. Absorbance was converted into moles of reducing sugars produced. One unit of enzyme activity was defined as 1 μmol of xylose released/min. at 60°C.

To determine the optimum pH for the xylanases, the assays were performed as described above except that sodium phosphate and citric acid buffers were used to generate a pH range from 3 to 8 (XynA and XynC assays were done at 70°C and XynB assays at 60°C). The effect of pH on enzyme stability was determined using the same buffer system to generate a pH range of pH 3 to pH 8; however, the enzymes were incubated for 2 hours at 30°C before activity was assayed. Xylanase temperature optima were determined by assaying the amount of reducing sugar ends produced at pH 4.5 at various temperatures. Effect of temperature on enzyme stability was determined by incubating the enzymes for 30 min. at different temperatures prior to performing the enzyme assay as described above.

Kinetic studies were performed at the pH and temperature optima for each xylanase using birchwood xylan (1 to 10 mg/mL), for which enzyme reactions followed Michaëlis-Menten kinetics. The K_m and the V_{max} were determined using Lineweaver-Burk plots.

3.8 Substrate specificity and heavy metal inhibitors

Substrate specificity of the three xylanases was tested using three natural substrates, birchwood xylan, oatspelt xylan and beechwood xylan (Sigma); CMC (carboxymethyl-cellulose), *p*-nitrophenyl- β-D-xylopyranoside ($pNPX_2$ from Sigma); and *p*-nitrophenyl-β-D-cellobioside ($pNPC_2$ from Sigma).

Enzyme assays using the natural substrates and CMC were performed as described above. Enzyme assays using $pNPC_2$ and $pNPX_2$ were performed as follows: enzymes were

incubated with substrates at a final concentration of 2 mg/mL in a total volume of 100 µL in NaAc, 50 mM, pH 4.5. The reactions were stopped with 900 µL of Na_2CO_3 (0.1 M) and the absorbance was read at 410 nm.

The inhibitory effect of Cu^{2+}, Zn^{2+}, Mg^{2+}, Hg^{2+} and Pb^{2+} on enzyme activity was tested by including 2 mM for each heavy metal in the aforementioned assays.

3.9 Analysis of xylan, xylopentaose, xylotriose and xylobiose degradation products by thin layer chromatography (TLC)

Birchwood xylan, xylopentaose (Megazyme), xylotriose (Megazyme), and xylobiose (Megazyme) hydrolysis was carried out in 100 µL reaction volumes. Each xylanase (6 U/mL) was added to a 1% solution of each substrate and incubated at 37°C. Ten to fifteen µL of each reaction mixture was analyzed by way of silica gel TLC (Sigma) with chloroform-acetic acid-water (6:7:1, [v/v]) as the solvent system. Reaction products were visualized by spraying a sulfuric acid-ethanol (5:95 [v/v]) solution on the plate followed by baking for 10 minutes at 110°C (Blanco *et al.*, 1999).

3.10 DNA sequencing

The complete DNA sequence of all nine xylanase clones was determined using a primer walking strategy. The individual sequencing reactions were processed by the McGill University and Genome Quebec Innovation Centre (McGill University). Each xylanase insert was completely sequenced on both strands and their sequences generated by assembling the overlapping sequences.

4. Results

4.1 Sequence analysis of the three xylanases

We searched the publicly available *P. chrysosporium* genome sequence using tblastn to identify potential xylanase genes and selected three gene sequences, *xynA*, *xynB* and *xynC*. First we analyzed the deduced amino acid sequences of their proteins using CDART and Scanprosite. CDART detected a glycosyl hydrolase family 10 domain in both XynA and XynC (Fig. 4.1.1A), a glycosyl hydrolase family 11 domain in XynB (Fig. 4.1.1B) and a fungal carbohydrate binding domain (fCBD) in all three proteins (Fig. 4.1.1C). The predicted fCBDs were very similar and typical of previously described fCBDs (Fig 4.1.1C). These are small domains of 33-40 contiguous amino acids arranged in three antiparallel β-strands that bind cellulose. fCBDs are believed to act by increasing the concentration of enzymes on the substrate without affecting the catalytic properties. The carbohydrate binding and catalytic domains in each xylanase were separated by a short 40 to 50 residue low complexity region rich in serine, threonine and proline (Fig. 4.1.1A and B). These linker regions are believed to provide flexibility (Black *et al.*, 1996) thereby allowing the fCBD and catalytic domain to simultaneously interact with cellulose and the substrate. Scanprosite detected a conserved active site motif typical of family 10 glycosyl hydrolases in both XynA and XynC (Fig. 4.1.1A) and the bipartite active site signature typical of family 11 hydrolases in XynB (Fig. 4.1.1B).

Alignments of the deduced xylanase sequences with other family 10 and 11 xylanases (Fig. 4.1.1A and 4.1.1B) found that 105 of the 309 residues within the conserved catalytic domains of the 5 family 10 member proteins and 62 of the 185 catalytic domain residues

Figure 4.1.1 Sequences alignments of xylanases. A. Alignment of *P. chrysosporium* XynA and XynC with family 10 xylanases, XlnA from *Agaricus bisporus* (CAB05665), XynA from *A. niger* (JT0608) and XynA from *Thermoascus aurantiacus* (AAF24127). B. Alignment of *P. chrysosporium* XynB with family 11 xylanases, Xynp1 from *Penicillium sp.* (JC7307), Xyn11a from *Lentinula edodes* (AAL04152) and XynA from *Bacillus subtilis* (CAA84276). C. Alignment of predicted fCBDs from *P. chrysosporium* XynA, XynB and XynC with other type I CBDs, from *Trichoderma reesei* Cip2 (AAP57749), *T. reesei* CBHII (AAG39980) and *A. bisporus* CBH (P49075). For Panel A and B, conserved active site motifs and fCBDs are enclosed in solid and dashed boxes, respectively. Low complexity linker regions are indicated by horizontal arrows and active site glutamates are indicated by vertical arrows. Catalytic domains identified by CDART extend from residues 102 to 411 for XynA and from residues 42 to 227 for XynB.

A

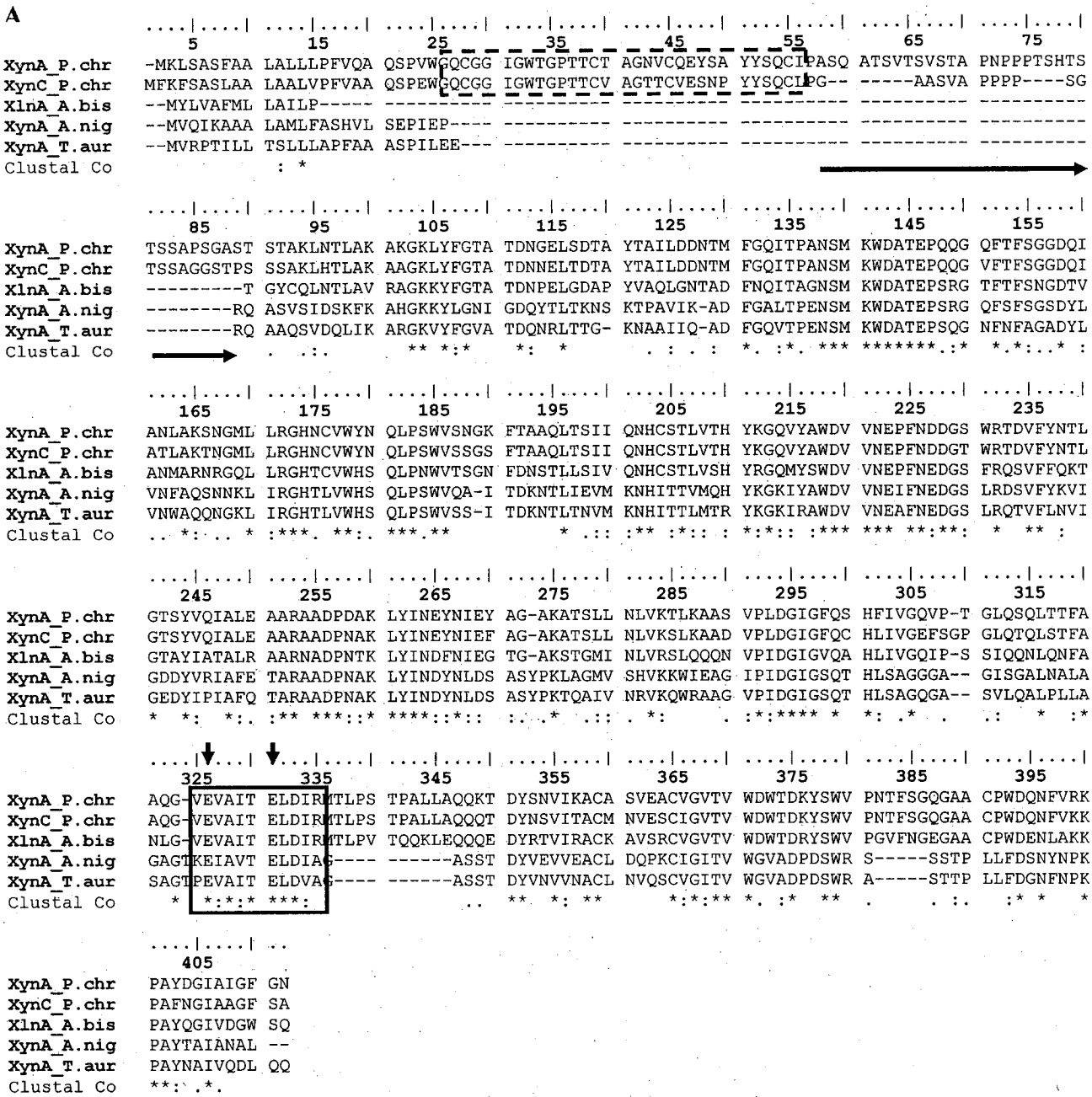
5 15 25 35 45 55 65 75
XynA_P.chr -MKLSASFAA LALLLPFVQA QSPVWGQCGG IGWTGPTTCT AGNVCQEYSA YYSQCLPASQ ATSVTSVSTA PNPPPTSHTS
XynC_P.chr MFKFSASLAA LAALVPFVAA QSPEWGQCGG IGWTGPTTCV AGTTCVESNP YYSQCLPG-- -----AASVA PPPP----SG
XlnA_A.bis --MYLVAFML LAILP----- ---------- ---------- ---------- ---------- ---------- ----------
XynA_A.nig --MVQIKAAA LAMLFASHVL SEPIEP---- ---------- ---------- ---------- ---------- ----------
XynA_T.aur --MVRPTILL TSLLLAPFAA ASPILEE--- ---------- ---------- ---------- ---------- ----------
Clustal Co : *
85 95 105 115 125 135 145 155
XynA_P.chr TSSAPSGAST STAKLNTLAK AKGKLYFGTA TDNGELSDTA YTAILDDNTM FGQITPANSM KWDATEPQQG QFTFSGGDQI
XynC_P.chr TSSAGGSTPS SSAKLHTLAK AAGKLYFGTA TDNNELTDTA YTAILDDNTM FGQITPANSM KWDATEPQQG VFTFSGGDQI
XlnA_A.bis ---------T GYCQLNTLAV RAGKKYFGTA TDNPELGDAP YVAQLGNTAD FNQITAGNSM KWDATEPSRG TFTFSNGDTV
XynA_A.nig --------RQ ASVSIDSKFK AHGKKYLGNI GDQYTLTKNS KTPAVIK-AD FGALTPENSM KWDATEPSRG QFSFSGSDYL
XynA_T.aur --------RQ AAQSVDQLIK ARGKVYFGVA TDQNRLTTG- KNAAIIQ-AD FGQVTPENSM KWDATEPSQG NFNFAGADYL
Clustal Co . .:. ** *:* *: * . : . : *. :*. *** *******.:* *.*:..* :
165 175 185 195 205 215 225 235
XynA_P.chr ANLAKSNGML LRGHNCVWYN QLPSWVSNGK FTAAQLTSII QNHCSTLVTH YKGQVYAWDV VNEPFNDDGS WRTDVFYNTL
XynC_P.chr ATLAKTNGML LRGHNCVWYN QLPSWVSSGS FTAAQLTSII QNHCSTLVTH YKGQVYAWDV VNEPFNDDGT WRTDVFYNTL
XlnA_A.bis ANMARNRGQL LRGHTCVWHS QLPNWVTSGN FDNSTLLSIV QNHCSTLVSH YRGQMYSWDV VNEPFNEDGS FRQSVFFQKT
XynA_A.nig VNFAQSNNKL IRGHTLVWHS QLPSWVQA-I TDKNTLIEVM KNHITTVMQH YKGKIYAWDV VNEIFNEDGS LRDSVFYKVI
XynA_T.aur VNWAQQNGKL IRGHTLVWHS QLPSWVSS-I TDKNTLTNVM KNHITTLMTR YKGKIRAWDV VNEAFNEDGS LRQTVFLNVI
Clustal Co .. *:. .. * :***. **:. ***.** * .:: :** :*:: : *:*:: :*** *** **:**: * ** :
245 255 265 275 285 295 305 315
XynA_P.chr GTSYVQIALE AARAADPDAK LYINEYNIEY AG-AKATSLL NLVKTLKAAS VPLDGIGFQS HFIVGQVP-T GLQSQLTTFA
XynC_P.chr GTSYVQIALE AARAADPNAK LYINEYNIEF AG-AKATSLL NLVKSLKAAD VPLDGIGFQC HLIVGEFSGP GLQTQLSTFA
XlnA_A.bis GTAYIATALR AARNADPNTK LYINDFNIEG TG-AKSTGMI NLVRSLQQQN VPIDGIGVQA HLIVGQIP-S SIQQNLQNFA
XynA_A.nig GDDYVRIAFE TARAADPNAK LYINDYNLDS ASYPKLAGMV SHVKKWIEAG IPIDGIGSQT HLSAGGGA-- GISGALNALA
XynA_T.aur GEDYIPIAFQ TARAADPNAK LYINDYNLDS ASYPKTQAIV NRVKQWRAAG VPIDGIGSQT HLSAGQGA-- SVLQALPLLA
Clustal Co * *: *:. :** ***::* ****::*:: :. .* .:: . *: . :*:**** * *: .* . .: * :*
325 335 345 355 365 375 385 395
XynA_P.chr AQG-VEVAIT ELDIRMTLPS TPALLAQQKT DYSNVIKACA SVEACVGVTV WDWTDKYSWV PNTFSGQGAA CPWDQNFVRK
XynC_P.chr AQG-VEVAIT ELDIRMTLPS TPALLAQQQT DYNSVITACM NVESCIGVTV WDWTDKYSWV PNTFSGQGAA CPWDQNFVKK
XlnA_A.bis NLG-VEVAIT ELDIRMTLPV TQQKLEQQQE DYRTVIRACK AVSRCVGVTV WDWTDRYSWV PGVFNGEGAA CPWDENLAKK
XynA_A.nig GAGTKEIAVT ELDIAG---- ------ASST DYVEVVEACL DQPKCIGITV WGVADPDSWR S-----SSTP LLFDSNYNPK
XynA_T.aur SAGTPEVAIT ELDVAG---- ------ASST DYVNVVNACL NVQSCVGITV WGVADPDSWR A-----STTP LLFDGNFNPK
Clustal Co * *:*:* ***: .. ** *: ** *:*:** *. :* ** . . :. :* * *
405
XynA_P.chr PAYDGIAIGF GN
XynC_P.chr PAFNGIAAGF SA
XlnA_A.bis PAYQGIVDGW SQ
XynA_A.nig PAYTAIANAL --
XynA_T.aur PAYNAIVQDL QQ
Clustal Co **: .*.

B

```
                 ....|....| ....|....| ....|....| ....|....| ....|....| ....|....| ....|....| ....|....| ....|....|
                      5         15         25         35         45         55         65         75
XynB_P.chr       MVSFNSLLVA VSAATCALAF PFEFHNGTHV FPRQSTPAGT GTNNGYFYSF WTDGGGSVTY NNGPAGEYSV TWSNADNFVA
Xynp1_P.sp       MKSFIAYLLA SVAVTGVMAV PGEYHK-RHD KRQTITSSQT GTNNGYYYSF WTNGGGTVQY TNGAAGEYSV TWENCGDFTS
Xyn1_T.ree       MVSFTSLLAA SPPSRASCRP AAEVESVAVE KRQTIQP-GT GYNNGYFYSY WNDGHGGVTY TNGPGGQFSV NWSNSGNFVG
Xyn11a_L.e       -MAYKSLLFL ALIAVTATAL D-VFDNSTEV IGKRSIPNGE GTNNGYFYSV YSDTTVTGTY TNGPGGEYTL TWGGSGDVVV
XynA_B.sub       MFKFKKNFLV GLS------- -------AAL MSISLFSATA SAASTDYWQN WTDGGGIVNA VNGSGGNYSV NWSNTGNFVV
Clustal Co          :   :                          .   . .  ::.  :.:         **..*:::: .* . .:..

                 ....|....| ....|....| ....|....| ....|....| ....|....| ....|....| ....|....| ....|....| ....|....|
                      85         95        105        115        125        135        145        155
XynB_P.chr       GKGWNPGS-A QAISF-TANY QPNGNSYLSV YGWSTNPLVE YYILEDYGTY NPAVSLTHKG TLTSDGATYD VYEGTRVNEP
Xynp1_P.sp       GKGWSTGS-A RDITF-EGTF NPSGNAYLAV YGWTTSPLVE YYILEDYGDY NPGNSMTYKG TVTSDGSVYD IYEHQQVNQP
Xyn1_T.ree       GKGWQPGTKN KVINF-SGSY NPNGNSYLSV YGWSRNPLIE YYIVENYGTY NPSTGATKLG EVTSDGSVYD IYRTQRVNQP
Xyn11a_L.e       GKGWNPGG-P MSVEY-SGTY SPNGNSYLSV YGWMTSPLVE YYITDSYGDY NPSTGGTHLG TCTSDGGVYD IYTQTRTNAP
XynA_B.sub       GKGWTTGSPF RTINYNAGVW APNGNGYLTL YGWTRSPLIE YYVVDSWGTY RPTG--TYKG TVKSDGGTYD IYTTTRYNAP
Clustal Co       **** .*      : :  . :  *.**.**:: *** .**:* **: :.:* * .*    *  *   .***..** :*   : * *

                 ....|....| ....|....| ....|....| ....|....| ....|....| ....|....| ....|....| ....|....| ....|....|
                     165        175        185        195        205        215        225        235
XynB_P.chr       SIQG-TATFN QYWSIRSSKR SSG---TVTT ANHFAAWKQL GLPLGT-FNY QIVATEGYQS SGSSTVTVNP AGGVTSPTAP
Xynp1_P.sp       SISG-TATFN QYWSIRQNTR SSG---TVTT ANHFNAWAKL GMNLGS-FNY QIVSTEGYES SGSSTITVS- ----------
Xyn1_T.ree       SIIG-TATFY QYWSVRRNHR SSG---SVNT ANHFNAWAQQ GLTLGT-MDY QIVAVEGYFS SGSASITVS- ----------
Xyn11a_L.e       SIQG-TATFQ QYWSIRQTHR VGG---TVTT GNHYSCWESV GLPLGT-FNY IILATEGYSS SGTSTITVG- QGTGTGSSAP
XynA_B.sub       SIDGDRTTFT QYWSVRQSKR PTGSNATITF TNHVNAWKSH GMNLGSNWAY QVMATEGYQS SGSSNVTVW- ----------
Clustal Co       ** *  :**  ****:* . *   *   ::.   **  .* .  *: **:   *  :::.*** * **::  :**

                 ....|....| ....|....| ....|....| ....|....| ....|....| ....|...
                     245        255        265        275        285        295
XynB_P.chr       TGPSSVSTTP SGPSSSPSPV GSCAALYGQC GGQGWTGPTC CSS-GTCKFS NNWYSQCL
Xynp1_P.sp       ---------- ---------- --------L- ---------- ---------- --------
Xyn1_T.ree       ---------- ---------- --------L- ---------- ---------- --------
Xyn11a_L.e       SGPSSTTTTP P-----TAPT GGTVAQWGQC GGIGYSGPTT CASPYTCTVA NAYYSQCL
XynA_B.sub       ---------- ---------- ---------- ---------- ---------- --------
Clustal Co
```

C

```
                 ....|....| ....|....| ....|....| .
                      5         15         25
XynA_P.chr       GQCGGIGWTG PTTCTAGNVC QEYSAYYSQC I
Cip2_T.ree       GQCGGIGWSG PTTCVGGATC VSYNPYYSQC I
XynC_P.chr       GQCGGIGWTG PTTCVAGTTC VESNPYYSQC L
XynB_P.chr       GQCGGQGWTG PTCCSSG-TC KFSNNWYSQC L
CBHII_T.re       GQCGGQNWSG PTCCASGSTC VYSNDYYSQC L
CBH_A.bisp       GQCGGNGWTG PTTCASGSTC VKQNDFYSQC L
Clustal Co       ***** .*:* ** * .* .*    . :**** :
```

of the family 11 xylanases were strictly conserved (Fig. 4.1.1A and 4.1.1B). SignalP predicted that XynA, XynC and XynB were translated as preproteins that contain 19, 20 and 19 residue signal peptides. Without any post-translational modifications except for cleavage of the signal peptide, the predicted molecular weights were 41.6, 28.6 and 40.3 kDa for XynA, XynB and XynC, respectively. The predicted pIs were 5.8 for XynA, 6 for XynB and 5.5 for XynC.

The 3-D structures of the catalytic domains of the three xylanases were generated using template structures available from the Protein Data Bank (Berman *et al.* 2000). Five templates (1goqA, 1gokA, 1gooA, 1gomA and 1gorA) derived for the *Thermoascus aurantiacus* xylanase TaXynA were used to generate the XynA and XynC structures (Fig. 4.1.2A). TaXynA shares 50% sequence identity with both XynA and XynC. The predicted structures of the catalytic domains of both enzymes were eight-fold α/β barrel structures typical of the family10 xylanases (Davies and Henrissat, 1995). The 3-D structure for XynB (Fig. 4.1.2B) was generated using 5 templates (1redA, 1reeA, 1redB, 1enxB and 1reeB) derived from the *Trichoderma reesei* Xyn2 protein, which shares 64.5% sequence identity with the XynB catalytic domain. The predicted XynB catalytic domain is typical of family 11 structures which are principally composed of β-sheets (Davies and Henrissat, 1995). Furthermore, the modeled catalytic domain of XynB included a substrate binding site that was significantly more accessible than the substrate binding sites of the two family 10 xylanases.

Figure 4.1.2. Predicted ribbon structures of XynB and XynC. A. XynC catalytic domain. **B.** XynB catalytic domain. Flat and coiled ribbon structures represent β-strand and α-helix structures. The two catalytic glutamates, 313 and 318 for XynC and 118 and 204 for XynB, that are presented in stick format, are located within the predicted active site. The scale (bottom left) represents 5 Å. A model generated for the XynA catalytic domain (not shown) is essentially identical to XynC.

A

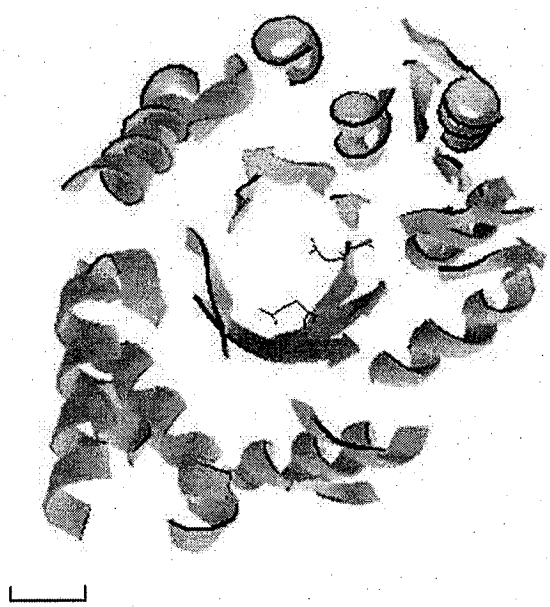

B

4.2 Cloning and testing for functional expression

The XynA, XynB and XynC DNAs obtained by PCR amplification of *P. chrysosporium* genomic DNA were estimated to be 1500, 950 and 1500 bp respectively (data not shown). These sizes were very close to the expected sizes (1524, 960 and 1501 bp) based on the sequenced *P. chrysosporium* genome. Three independent ANEp2 constructs harboring each xylanase gene were used to transform *A. niger* strain N593 and two independent *A. niger* transformants were assayed for xylanase expression. All 6 transformants harboring the same xylanase gene expressed similar levels of secreted xylanase, suggesting that the various manipulations had not introduced mutations that deleteriously affected either expression or enzymatic activity. Two transformants from each of the expressed xylanases were selected for detailed characterization.

4.3 Xylanase expression and purification

The three *A. niger* transformants (N593-ANEp2-xynA-1, N593-ANEp2-xynB-1 and N593-ANEp2-xynC-1), were grown in MM with maltose as the carbon source. After 48 h, the medium was harvested and dialyzed as described in the Materials and Methods. The secreted proteins produced by the three strains were assayed for xylanase activity. The results (Table 4.3.1) showed that no xylanase activity was detected in the culture medium of the control strain N593-ANEp2, whereas significant activity was expressed by the three other strains. The amount of XynB activity expressed was about 4.5 times higher than the amount of activity expressed by the XynA and XynC transformants.

Table 4.3.1 Secreted xylanase activity expressed by *A. niger* strain N593 harboring the plasmids indicated

Plasmid	Xylanase activity from crude samples (U/mL) [a]
ANEp2	0
ANEp2-xynA-1,2,3	0.47 ± 0.03
ANEp2-xynB-1,2,3	3.17 ± 0.06
ANEp2-xynC-1,2,3	1.22 ± 0.08

[a] Activity was determined as described in the Materials and Methods using filtered and dialyzed culture medium.

Since all three xylanases apparently harbored a fCBD, we used Avicell chromatography as a second step for XynA and XynB purification. After Avicell chromatography, the xylanases were obtained as pure proteins with estimated masses of 52 and 32 kDa for XynA and XynB (Fig 4.3.1A and 4.3.1B), respectively. This second purification step confirmed that both xylanases harbored functional fCBDs. XynC was purified using another method and its mass was estimated to be 50 kDa (Fig 4.3.1C).The experimentally determined molecular masses were significantly greater than predicted masses of 41.6, 28.6 and 40.3. Differences between the predicted and determined masses can be explained by post-translational modifications such as glycosylation. Supporting this possibility, several potential O-glycosylation sites were located in the linker regions of all three xylanases. There is also one potential N-glycosylation site near the N-terminal end of XynB.

To confirm that the purified proteins were indeed XynA, XynB and XynC, we performed MALDI mass spectrometry. The three purified xylanases were subjected to SDS-PAGE, digested by trypsin and peptide mapping of these fragments performed by mass-spectrometry confirmed the identity of the purified proteins (data not shown).

4.4 Characterization of XynA, XynC and XynB

Purified preparations of the three xylanases were also used to determine their biochemical properties. The two family 10 xylanases exhibited very similar biochemical properties. The *Km* values of XynA and XynC, 3.42 ± 0.69 and 3.71 ± 0.69 mg xylan/mL, respectively, were not significantly different. Both family 10 xylanases exhibited maximal activity at 70°C and at a pH of 4.5 (Fig 4.4.1A and 4.4.1B).

Figure 4.3.1 Results of the xylanase purifications. A. SDS-PAGE analysis of XynA extracts following 60% ammonium sulfate precipitation (lane 1) and Avicell chromatography (lane 2). **B.** SDS-PAGE analysis of XynB extracts following 80% ammonium sulfate precipitation (lane 1) and Avicell chromatography (lane 2). **C.** Analysis of fractions obtained following the DEAE step of XynC purification. SDS-PAGE performed on fractions 10 to 16 (upper panel) and xylanase activity determined by DNSA assays, on fractions 11 to 15 (lower panel).

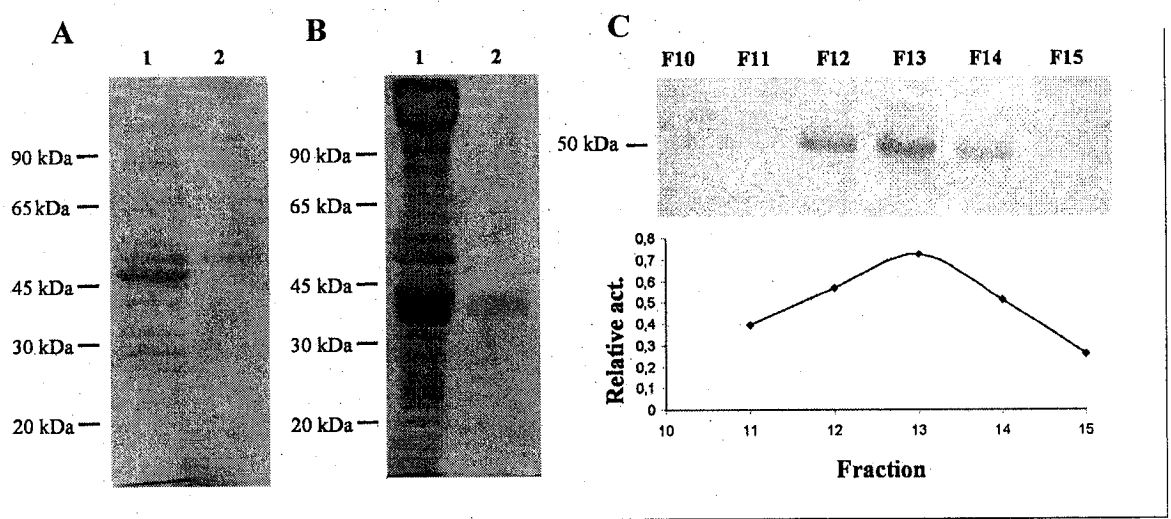
A
1
2
90 kDa
65 kDa
45 kDa
30 kDa
20 kDa
B
1
2
90 kDa
65 kDa
45 kDa
30 kDa
20 kDa
C
F10
F11
F12
F13
F14
F15
50 kDa
Relative act.
0,8
0,7
0,6
0,5
0,4
0,3
0,2
0,1
0
10
11
12
13
14
15
Fraction

Figure 4.4.1 Biochemical properties of the *P. chrysosporium* xylanases. A. Effect of temperature on xylanase activity. **B.** Effect of pH on activity. **C.** Effect of 30 min. preincubations at the temperatures indicated on activity. For Panel A-C, closed triangles represent XynA, closed circles represent XynB and closed squares XynC. **D.** Relative activity of each xylanase toward various substrates where activities on oatspelt xylan represent 100%. Oatspelt, beechwood and birchwood xylan are indicated as Oat, Bee and Bir.

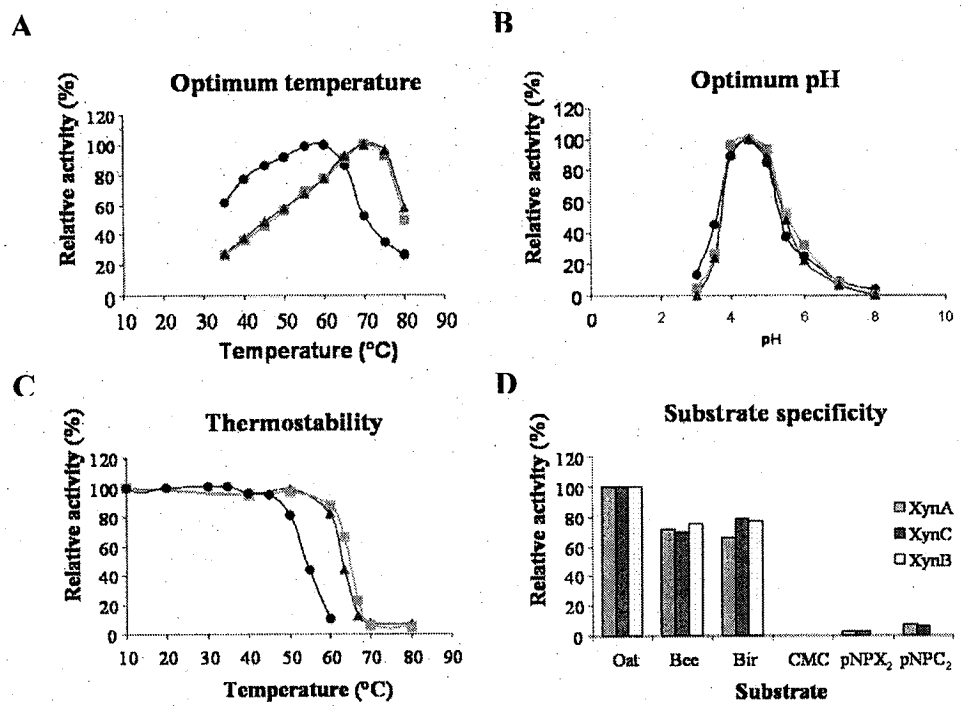
A
Optimum temperature
Relative activity (%)
120
100
80
60
40
20
0
10 20 30 40 50 60 70 80 90
Temperature (°C)
B
Optimum pH
Relative activity (%)
120
100
80
60
40
20
0
0 2 4 6 8 10
pH
C
Thermostability
Relative activity (%)
120
100
80
60
40
20
0
10 20 30 40 50 60 70 80 90
Temperature (°C)
D
Substrate specificity
Relative activity (%)
120
100
80
60
40
20
0
XynA
XynC
XynB
Oat
Bee
Bir
CMC
pNPX2
pNPC2
Substrate

Neither XynA nor XynC lost significant activity during a 30 min pre-incubation at 60°C; however, they were completely inactivated by a pre-incubation at 70°C (Fig. 4.4.1C). pH stability assays found no significant loss of activity for XynA during two hour pretreatments ranging from pH 3 to pH 8 (data not shown). Substrate specificity assays found that XynA and XynC hydrolyze oatspelt xylan slightly better than beechwood or birchwood. Both XynA and XynC were able to weakly hydrolyze the synthetic substrates $pNPX_2$ and $pNPC_2$ but did not hydrolyze CMC (Fig 4.4.1D). Activity assays performed in the presence of different heavy metals found that only Pb^{2+} and Hg^{2+} inhibited XynA and XynC at the concentration tested. Pb^{2+} at 2 mM acted as a weak inhibitor of XynA and XynC, since they retained about 70% of their activity when assayed in its presence. The presence of 2 mM Hg^{2+} strongly inhibited both XynA and XynC reducing their activity by about 80%.

The biochemical properties of the family 11 xylanase, XynB, were also determined. Its *Km* was 9.96 ± 1.45 mg/mL when birchwood xylan was used as substrate. XynB exhibited maximal activity at 60°C and pH 4.5 (Fig. 4.4.1A and 4.4.1B). Thermostability assays found XynB was stable at 50°C but unstable at 70°C for the same incubation time (Fig. 4.4.1C). No significant loss of activity was observed after 2 hours of incubation at pHs ranging from 3 to 8 (data not shown). XynB exhibited a higher activity on oatspelt xylan than on beechwood and birchwood xylans and no activity was detected with the polysaccharide CMC nor the synthetic substrates $pNPX_2$ and $pNPC_2$ (Fig. 4.4.1D). Both Pb^{2+} and Hg^{2+} acted as weak inhibitors, since XynB retained about 80% of its activity in presence of Pb^{2+} and 67% of its activity when assayed in the presence of Hg^{2+}.

4.5 Ability of the three xylanases to hydrolyze xylose polymers

XynA and XynC exhibited essentially identical enzymatic characteristics with regard to their abilities to degrade the various xylose polymers; therefore we have presented the results for only one G-H family 10 xylanase in each panel of Figure 4.5.1. The family 10 xylanases degraded small but detectable amounts of xylotriose, but neither xylobiose nor xylotriose were efficiently degraded. Both family 10 xylanases degraded xylotetraose producing mainly xylobiose. Of the xylooligosaccharides tested, the most efficiently hydrolyzed was xylopentaose. It was converted mainly to xylobiose and xylotriose, although a majority of xylopentaose was converted to xylobiose. Birchwood xylan hydrolysis by the family 10 members produced products, which showed chromatographic mobility similar to xylobiose, xylotriose, xylotetraose and xylopentaose; however, two major products accumulated after incubation for 24 hours. These migrated with a mobility similar to xylobiose and xylotetraose (Fig 4.5.1B), suggesting these were the major end products. Products released during the hydrolysis of two other xylans were not significantly different than those produced from birchwood xylan (Fig. 4.5.1B).

XynB did not hydrolyze xylobiose or xylotriose under the assay conditions tested. The family 11 xylanase did convert xylotetraose into xylobiose and xylotriose, and xylopentaose mainly into xylobiose and a small amount of xylotriose (Fig. 4.5.1A). Weak polymerase activity resulting in the production of xylose polymers with degrees of polymerization (D.P.) > 3 and > 4 were detected when xylotriose and xylotetraose were the substrates. Degradation of birchwood xylan by XynB produced results significantly different than that obtained with the family 10 xylanases (Fig. 4.5.1B).

Figure 4.5.1 TLC analyses of reaction products. A. Products released during a 16h incubation of xylobiose (X2), xylotriose (X3) and xylopentaose (X5) with XynA and XynB as indicated (left panel), and products released from xylotetraose (X4) following incubation with XynB and XynC (right panel). **B.** XynA and XynB were incubated with 1% birchwood xylan for the time indicated (left panel). Products released from birchwood, beechwood and oatspelt xylan incubated for 24 hours with XynB and XynC as indicated (right panel). The standards used were xylose (X1), xylobiose (X2), xylotriose (X3), xylotetraose (X4) and xylopentaose (X5).

A

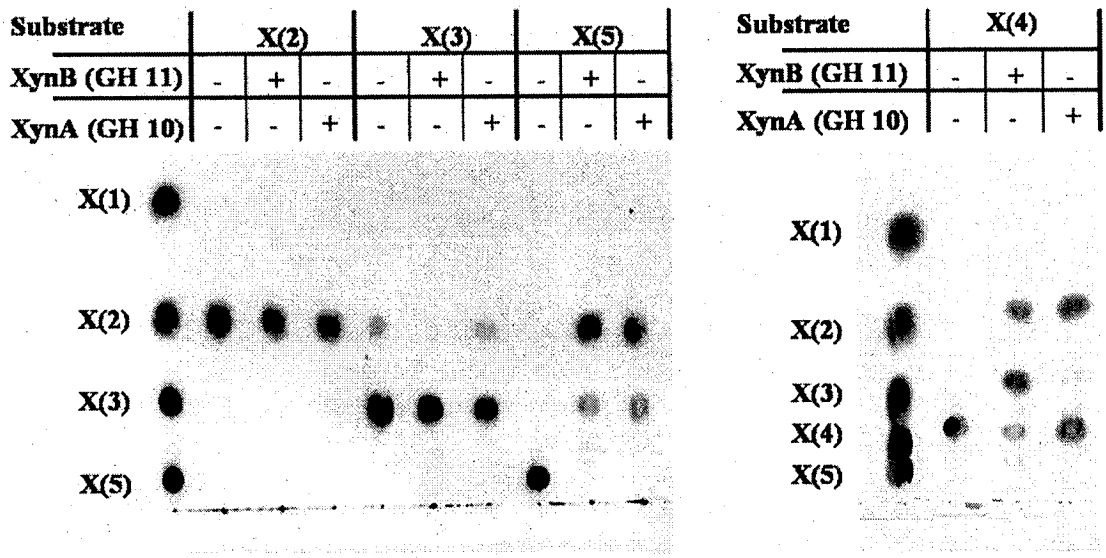
Substrate
X(2)
X(3)
X(5)
XynB (GH 11)
XynA (GH 10)
X(1)
X(2)
X(3)
X(5)
Substrate
X(4)
XynB (GH 11)
XynA (GH 10)
X(1)
X(2)
X(3)
X(4)
X(5)

B

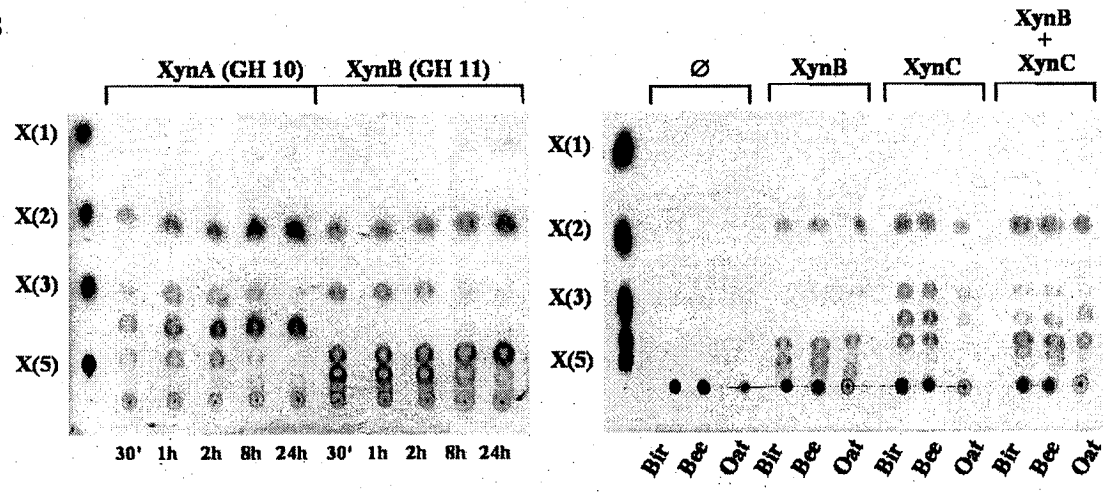
XynA (GH 10)
XynB (GH 11)
X(1)
X(2)
X(3)
X(5)
30' 1h 2h 8h 24h 30' 1h 2h 8h 24h
∅
XynB
XynC
XynB + XynC
X(1)
X(2)
X(3)
X(5)
Bir Bee Oat Bir Bee Oat Bir Bee Oat Bir Bee Oat

The four principal products detected at intermediate times during hydrolysis showed chromatographic mobility similar to xylobiose, xylotriose, xylopentaose and a xylooligosaccharide with a D.P.>5; however, after 24 hours of hydrolysis the two major products that remained showed mobility similar to xylobiose and xylopentaose. Degradation products from beechwood and oatspelt xylan were not significantly different that those produced from birchwood xylan (Fig. 4.5.1B).

4.6 Sequencing results

We determined the DNA sequence of three independent clones of *xynA, xynB* and *xynC*. Tables 4.6.1A, 4.6.2A and 4.6.3A report all the nucleotide differences observed between the three *xynA*, *xynB* and *xynC* DNA sequences, respectively. These sequences were also compared with the two *P. chrysosporium* genome sequences available at the US Department of Energy Joint Genome Institute (JGI) website (http://genome.jgi-psf.org/whiterot1/whiterot1.home.html) provided in the August 2002 and March 2004 releases, respectively. Tables 4.6.1B, 4.6.2B and 4.6.3B present the amino acid differences observed between the five XynA, XynB and XynC proteins encoded by these sequences. The nucleotide sequences of my *xynA-1*, *xynA-2* and *xynA*-3 clones differed from the JGI *xynA* sequence by 12, 20 and 47 nucleotide differences, respectively. Remarkably only one of these 79 nucleotide differences altered the predicted sequence of the encoded protein. This one nucleotide difference altered XynA-2 such that residue 199 was a threonine rather than an asparagine (Fig. 4.6.1B).

Table 4.6.1 A. Comparison of the nucleotide sequences of the three independent xynA clones obtained and the two xynA sequences retrieved from the JGI 2002 and 2004 releases of the P. chrysosporium genome. [a] Nucleotide differences relative to the *xynA* sequence in the JGI 2002 genome sequence are designated as either silent (no effect on the XynA amino acid sequence) or missense (altered the amino acid sequence). For missense substitutions the amino acid in the JGI 2002 sequence and the substituted amino acid in the proteins encoded by clones described here and in the JGI 2004 sequence also are indicated using the single letter amino acid code.

Table 4.6.1 B. Comparison of the derived amino acid sequences of the XynA proteins encoded by the two JGI genomic sequences and clones *xynA-1, xynA-2, xynA-3*.

Figure 4.6.1. Location on the modeled XynA structure of the amino acid differences encoded by the XynA-2 clone.

Nucleotide position	Scaf74-02	Scaf74-04	*xynA-1*	*xynA-2*	*xynA-3*	Type of mutation[a]
12	A	-	T	T	T	Silent
51	G	-	-	-	A	Silent
54	G	-	-	-	A	Silent
66	T	-	-	-	C	Silent
94	G	-	-	-	A	Silent
102	A	-	-	-	G	Silent
104	A	-	-	-	C	Silent
111	G	-	-	-	T	Silent
167	T	-	-	-	C	Silent
221	C	-	-	-	T	Silent
231	C	-	-	-	T	Silent
239	G	-	-	-	A	Silent
247	C	-	-	-	A	Silent
250	T	-	-	-	C	Silent
254	C	-	-	-	T	Silent
256	C	-	-	-	T	Silent
257	C	-	-	-	G	Silent
325	T	-	-	G	G	Silent
328	G	-	-	C	C	Silent
361	C	-	T	T	T	Silent
368	C	-	-	A	A	Silent

Nucleotide position	**Scaf74-02**	**Scaf74-04**	*xynA-1*	*xynA-2*	*xynA-3*	**Type of mutation**[a]
412	C	-	-	-	A	Silent
436	G	-	-	-	C	Silent
481	T	-	-	-	C	Silent
534	A	-	-	-	G	Silent
544	C	-	-	-	T	Silent
550	A	-	-	-	C	Silent
555	T	-	-	-	C	Silent
556	G	-	-	-	A	Silent
567	T	-	-	-	C	Silent
568	A	-	-	-	G	Silent
569	C	-	-	-	G	Silent
572	A	-	-	-	C	Silent
579	T	-	-	-	C	Silent
581	C	-	-	-	T	Silent
593	C	-	-	-	T	Silent
682	G	-	T	T	T	Silent
808	G	-	-	C	-	Silent
814	C	-	-	T	-	Silent
820	A	-	-	G	-	Silent
822	A	-	-	C	-	**N/T**
844	C	-	-	G	-	Silent

Nucleotide position	Scaf74-02	Scaf74-04	*xynA-1*	*xynA-2*	*xynA-3*	Type of mutation[a]
868	C	-	-	T	-	Silent
874	C	-	-	T	-	Silent
964	C	-	T	T	T	Silent
1096	C	-	T	T	T	Silent
1141	G	-	T	T	T	Silent
1165	A	-	G	G	G	Silent
1351	A	-	G	G	G	Silent
1402	C	-	T	T	T	Silent
1407	T	-	-	DEL	DEL	Silent
1413	A	-	T	-	T	Silent
1427	G	-	T	-	-	Silent
1434	A	-	-	-	G	Silent
1435	C	-	G	-	G	Silent
Total	**55**	**0**	**12**	**20**	**47**	**1**

Amino acid position	Scaf74-02	Scaf74-04	XynA-1	XynA-2	XynA-3
200	N	-	-	T	-
Total	**1**	**-**	**-**	**1**	**-**

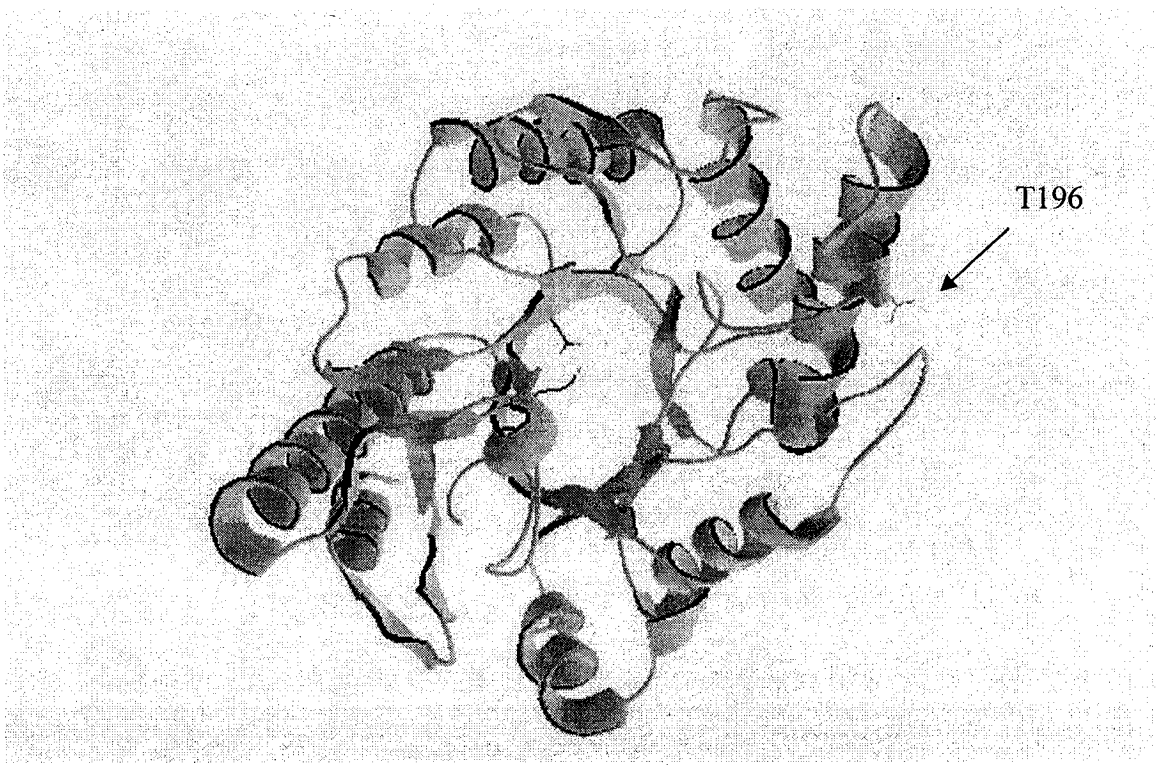
T196

Table 4.6.2 A. Comparison of the nucleotide sequences of the three independent *xynB* clones obtained and the two *xynB* sequences retrieved from the JGI 2002 and 2004 releases of the *P. chrysosporium* genome.

[a] Nucleotide differences relative to the *xynB* sequence in the JGI 2002 genome sequence are designated as either silent (no effect on the XynA amino acid sequence) or missense (altered the amino acid sequence). For missense substitutions the amino acid in the JGI 2002 sequence and the substituted amino acid encoded by the clones described here and the JGI 2004 sequence also are indicated using the single letter amino acid code.

Table 4.6.2 B. Comparison of the derived amino acid sequences of the XynB proteins encoded by the two JGI genomic sequences and clones *xynB-1, xynB-2, xynB-3*.

Nucleotide position	Scaf120-02	Scaf120-04	*xynB-1*	*xynB-2*	*xynB-3*	Type of mutation[a]
60	T	C	-	C	-	Silent
78	C	-	-	-	T	Silent
141	T	C	-	C	-	Silent
301	C	-	-	T	-	Silent
491	C	-	T	-	-	Silent
500	A	G	G	G	G	Silent
740	C	T	-	T	T	Silent
754	C	-	T	-	-	**T/I**
797	C	G	-	G	G	Silent
812	G	-	A	-	-	Silent
826	G	-	C	-	-	**S/T**
827	T	-	C	-	-	**S/T**
831	G	-	T	-	-	**A/S**
833	G	-	T	-	-	**A/S**
836	T	-	C	-	-	Silent
842	C	T	-	T	T	Silent
854	T	-	C	-	-	Silent
869	G	C	-	C	C	Silent
Total	**18**	**7**	**9**	**8**	**6**	**3**

Amino acid position	Scaf120-02	Scaf120-04	XynB-1	XynB-2	XynB-3
231	T	-	I	-	-
255	S	-	T	-	-
257	A	-	S	-	-
Total	**3**	**-**	**3**	**-**	**-**

Table 4.6.3 A. Comparison of the nucleotide sequences obtained for the three independent xynC clones obtained and the two xynC sequences retrieved from the JGI 2002 and 2004 releases of the P. chrysosporium genome. [a] Nucleotide differences relative to the *xynC* sequence in the JGI 2002 genome sequence are designated as either silent (no effect on the XynC amino acid sequence) or missense (altered the amino acid sequence). Missense substitutions, where the amino acid in the JGI 2002 sequence and the substituted amino acid in proteins encoded by the clones described here and the JGI 2004 sequence are indicated using the single letter amino acid code.

Table 4.6.3 B. Comparison of the derived amino acid sequences of the XynC proteins encoded by the two JGI genomic sequences and clones *xynC-1, xynC-2, xynC-3*.

Figure 4.6.2 Location on the modeled XynC structure of the amino acid differences encoded by *xynC-2* and *xynC-3* clones.

Nucleotide position	Scaf42-02	Scaf42-04	*xynC-1*	*xynC-2*	*xynC-3*	Type of mutation[a]
720	T	-	C	-	-	Silent
865	T	-	-	-	A	**F/I**
873	T	-	-	C	-	Silent
888	G	-	-	C	-	Silent
936	C	-	-	A	-	Silent
945	T	-	-	C	-	Silent
966	C	-	-	T	-	Silent
993	C	-	-	T	-	Silent
1071	C	-	-	T	-	Silent
1093	C	-	-	T	-	**L/F**
1461	C	-	-	-	A	Silent
Total	**11**	**0**	**1**	**8**	**2**	**2**

Amino acid position	Scaf42-02	Scaf42-04	XynC-1	XynC-2	XynC-3
214	F	-	-	-	I
290	L	-	-	F	-
Total	**2**	**0**	**0**	**1**	**1**

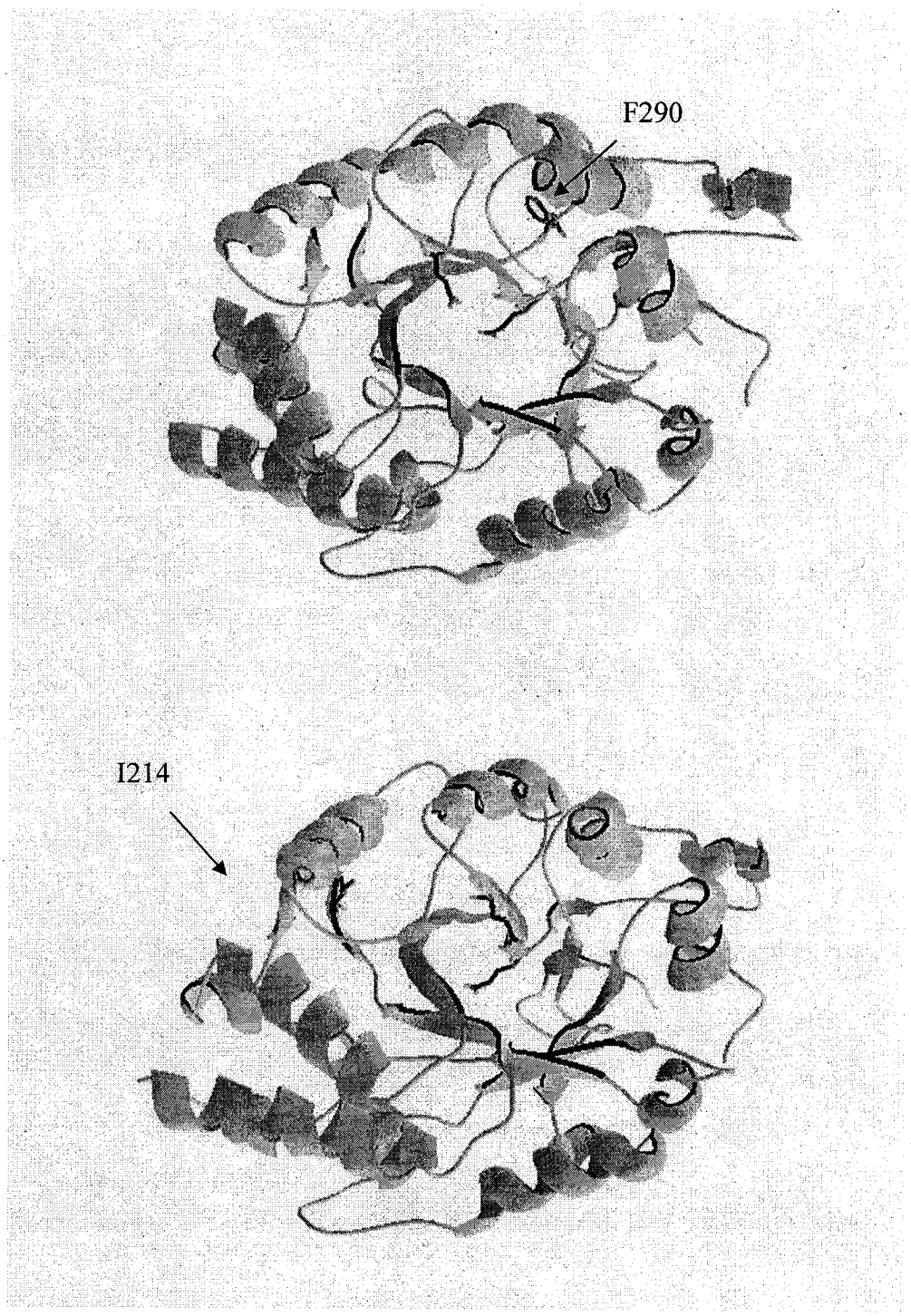
F290
I214

Based on the following arguments we feel that it is highly unlikely that the N196T substitution present the *xynA-2* allele significantly altered xylanase function. First, residue 196 is located on the protein surface in an α-helix far from the catalytic site (Fig. 4.6.1). Secondly, I found that the amount of xylanase activity expressed by *A. niger* transformants harboring the *xynA-2* clones was very similar to the amounts expressed by transformants harboring *xynA-1* and *xynA-3* clones. Further, an N to T substitution is fairly conservative and threonine residues occur at this position in other family 10 xylanases.

The number of nucleotide differences between the *xynB* clones described here and the scaffold 120-2002 sequence, ranged from 6 to 9 (Table 4.6.2), which is similar to the number of differences found between the *xynB* sequences available in the JGI 2002 and 2004 releases of the *P. chrysosporium* genome sequence. At the amino acid level, only the xylanase encoded by *xynB-2* was affected. This xylanase differed from those encoded by the *xynB-1, xynB-3* clones and *xynB* present in the JGI genome sequences at three amino residues, T231I, S255T and A257S (Table 4.6.3). All of these differences were located within the region of low sequence complexity linking the XynB catalytic and carbohydrate binding domains. Since tertiary structures have not been derived for these linker regions, it was impossible to locate these residues within a model structure for this portion of XynB.

As expected, the three linker region substitutions unique to XynB-1 did not adversely affect its encoded xylanase activity, since the linker region is a low complexity region rich in serine, threonine, alanine and proline residues that is not required for enzyme activity.

The nucleotide sequence of *xynC-1*, *xynC-2* and *xynC-3* differed from the *xynC* sequence present in the August 2002 and March 2004 versions of the *P. chrysosporium* genome sequence by 1, 8 and 2 single nucleotide differences, respectively (Table 4.6.5).Two of these

single base pair differences altered the XynC protein sequence. One generated a F214I substitution in XynC-2 and the other one resulted in a L290F substitution in XynC-3 (Fig. 4.6.3). The location of these two conservative substitutions is indicated in Figure 4.6.3C. For the same reasons evoked for XynA, it is not surprising that these two substitutions did not result in a detectable phenotype. In addition, both mutations are conservative amino acid substitutions (Henikoff and Henikoff, 1992).

5. Discussion

5.1 Identification of genes encoding xylanases in *Phanerochaete chrysosporium*

In this study, three *P. chrysosporium* xylanases have been characterized. Two additional xylanase genes have been identified in our laboratory. The genome of *P. chrysosporium* therefore codes for at least five xylanase genes. Among these five genes, four belong to G-H family 10 and one belongs to G-H family 11. This distribution is different from that found previously in other filamentous fungi where G-H family 11 xylanases predominate (Kulkarni *et al.*, 1999). The various approaches used to determine these ratios could actually be responsible for this divergence. For example, before genome sequences became available most studies characterized the secreted xylanases that were isolated from various culture media. This method is not systematic, because poorly expressed xylanases are difficult to detect and xylanase expression may be biased by the culture conditions used. In addition, alternative splicing and/or post-translational modifications can lead to an over-estimation of the number of xylanase genes. On the other hand, my approach only identified family 10 and 11 xylanases that were similar to those encoded by the query sequences used to perform the Blast searches. Another disadvantage of Blast-based gene identification is that it can only identify homologs of previously described genes.

5.2 Functional expression of xylanase

I successfully expressed three of the five *P. chrysosporium* xylanases in *A. niger*. XynA, XynB and XynC were functionally expressed at sufficient levels to allow me to purify and characterize them. The amount of xylanase activity expressed by *A. niger* during batch

culture growth peaked after about 48 hours. This contrasted with the pattern of native glucoamylase (Zito, 2003) and *P. chrysosporium* mannanase (Xiaoming Li, personal communications) expressed during batch culture growth by the same strain. Enzyme activity assays and SDS-PAGE analysis showed that both glucoamylase and mannanase continued to increase for at least 5 days and resulted in much higher levels of expression.

There are several possible explanations for the loss of xylanase activity following day 2 of batch culture growth. Proteolytic inactivation and pH induced instability are two obvious possibilities, because the amount of secreted protease activity increases dramatically and the pH decreases from about 7 units to 4 units between day two and day five of batch culture growth. My investigations determined that the three xylanases were stable during incubation at pH 4. Furthermore, the purified xylanases were stable when incubated with dialyzed day 3, 4 and 5 culture medium. Perhaps protease activity in culture medium is pH-dependent. Future studies directed at determining whether or not protease activity in the culture medium was inactivated during dialysis might explain why all three xylanases were stable in dialyzed culture medium.

I also tested the possibility that inefficient splicing contributed to the low levels of expression using ANEp2 derivatives that expressed cDNA clones for the three xylanases. The amount of xylanase activity expressed from these clones was similar to that obtained with the genomic DNA clones. Furthermore, the amount of xylanase activity present in culture filtrates decreased after day two in a fashion that was similar to that observed with the genomic DNA clones. These results show that intron excision was not adversely affecting expression of these heterologous genes.

Another possibility not explored in this study is that one or more intracellular events, such as translation, intracellular degradation or impaired secretion, contributed to the reduced xylanase expression observed during the latter stages of batch culture growth.

5.3 Characterization of *P. chrysosporium* xylanases

Several family 10 and 11 xylanases have been cloned, sequenced and subjected to biochemical characterization. Comparisons with previously characterized xylanases significantly facilitated my efforts to identify functional domains, locate catalytic sites and construct 3-D models.

Sapag *et al.* (2002) predicted that xylanases with pH optima below 5 would harbor an aspartate residue (D) at amino acid position 77 relative to the XynB primary sequence. XynB does not support this hypothesis, since it has an asparagine (N) at this position and a pH optimum of 4.5.

The *Km* of XynB was determined to be about three times higher than the *Km* of XynA and XynC. This suggests that the role of XynB in xylan degradation may be different than that of the two family 10 xylanases. Supporting this possibility, interesting differences were found among the three xylanases. The most striking difference was their differential action on xylotetraose. Xylotetraose was converted into xylobiose by XynA and XynC, whereas XynB produced both xylobiose and xylotriose. These differences can be attributed to less stringent binding of xylose oligomers by XynB, and the ability of XynB to perform transglycosylation reactions.

My xylan hydrolysis studies produced results that were similar to those reported in previous studies by Biely *et al.* (1997), Vardakou *et al.* (2003) and Christakopoulos *et al.* (2003). These authors found that family 11 xylanases produce aldopentauronic acid as the shortest

acidic fragment and family 10 xylanases produce aldotetrauronic acid. Biely *et al.* (1997) proposed that family 11 xylanases require xylose oligomers with at least 3 unsubstituted xylosyl residues to perform hydrolyses whereas family 10 xylanases require only 2 unsubstituted xylose residues.

Another feature that distinguishes family 10 xylanases from family 11 xylanases is the ability of family 10 xylanases to degrade short oligosaccharides such as $pNPX_2$ and $pNPC_2$ (Biely *et al.*, 1997). I also found that the two family 10 xylanases hydrolyzed $pNPC_2$ and $pNPX_2$, whereas the family 11 xylanase was unable to utilize these substrates.

5.4 Allelic differences of xylanases

The DNA sequence was determined for three independent *xynA*, *xynB* and *xynC* clones. Surprisingly, the sequence of all nine clones differed significantly from the nucleotide sequences of the *xynA, xynB* and *xynC* genes reported in both the 2002 and 2004 versions of the sequenced *P. chrysosporium* genome (http://genome.jgi-psf.org/whiterot1/whiterot1.home.html). Differences observed were numerous; however, only 6 out of the 70-nucleotide differences between the sequences presented here and the 2002 version of the genome sequence resulted in amino acid substitutions (Fig. 5.4.1, Fig. 5.4.2 and Fig. 5.4.3). The low number of amino-acid substitutions suggests that these differences have not occurred during gene amplification or some other cloning step. The simplest hypothesis is that the three clones are faithful copies of different allelic versions of the same gene. This assumption is reinforced by the observation that for xylanase B, all 7 nucleotide differences between the DOE's 2004 genome sequence and the reference sequence (2002 DOE release) are also present in at least one of the three *xynB* clones. T60C (where the first letter indicates the allele in the 2002 sequence and the second letter indicates the allele in the

2004 sequence) and T141C are found in *xynB*-2. C740T, C797G, C842T and G869C are common to both *xynB-2* and *xynB-3*, whereas A500G is shared by all three clones. That is, of the 18 differences between the sequences of these *xynB* clones and the 2002 release of the *P. chrysosporium* genome sequence 13 also are found in the 2004 version of the *P. chrysosporium* genome sequence.

It also is unlikely that the 84 nucleotide differences between the xylanase sequences in the 2002 release and the nine xylanase clones characterized in this study would have arisen during amplification and cloning. First, if these differences resulted from random events that occurred during PCR amplification, or cloning and propagation in *E. coli*, 75% should result in replacement mutations (mutations that result in changing one amino acid for another) versus 25% silent mutations. In these sequences, rather than the 63 replacement mutations expected by chance, only 6 replacement mutations were observed. The probability that this proportion of replacement mutations occurred by chance is $p < 0.0001$. One possible explanation is that the *P. chrysosporium* template DNA used in this study was isolated from a heterothallic strain and that the xylanase gene sequences available in the two releases of the *P. chrysosporium* genome (DOE Joint Genome Institute) are derived from sequencing reads that include various allelic version of the *P. chrysosporium* genes.

It might be useful to revaluate the homokaryotic character of strain RP 78 and to consider whether mitotic and/or meiotic recombination could also have contributed to the differences observed between the five sequences for these xylanase genes (summarized in Figure 5.4.2).

5.5 Potential application of *xynA, xynB and xynC* in the pulp and paper industry

The three xylanases I characterized had pH optima that were less than ideal for most pulp and paper industry applications (Nakamura *et al.*, 1993). However, they exhibited resistance to

heavy metals and the absence of cellulolytic activity, which are desirable traits. Although biobleaching mechanisms are still poorly understood, significant differences in biobleaching capabilities have been observed between various xylanases. Generally, G-H family 11 xylanases act more efficiently than do G-H family 10 members. This has been attributed to the smaller size of family 11 xylanases, which may facilitate access to the cellulosic network (Clarke *et al.*, 1997).

5.6 Perspective

Cloning and functional expression of all five *P. chrysosporium* xylanase genes would open up many interesting research fields, the most obvious one being studies directed at understanding the xylanolytic system of white rot fungi. Analysis of the five xylanase gene promoter regions might provide important clues about how these xylanases interact and the functional roles they play in xylan degradation. For example, the presence or lack of conserved upstream regulatory sequences may provide insight into how these xylanase genes are regulated including whether or not their expression is coordinately regulated. Xylan degradation also requires the action of several other enzymes such as xylosidases, α-L-arabinofuranosidases, acetylxylan esterases, α-glucuronidases and feruloyl esterases. These other enzymes and their genes might also be studied to fully understand how these other activities are regulated and how they interact to effect xylan degradation.

Another field of research might concern structure/function studies using site-directed mutagenesis. The accuracy of the 3-D models generated were found to be quite acceptable: the probability that the structures deviated from the correct structures by less than 3 Å was 79% for XynA and XynC and 85% for XynB (Chothia *et al.*, 1986, Harrison *et al.*, 1995,

Guex *et al.*, 1997 an Bajorath *et al.*, 1993). It should, therefore, be possible to use these structures to select specific residues for site-directed mutagenesis aimed at the rational design of mutants with improved characteristics for various commercial applications.

Finally, the fCBDs also could be investigated, since their functional roles in cellulose and hemicellulose degradation remain to be elucidated. One possibility would be to compare the activity of the XynA, XynB and XynC enzymes with and without their carbohydrate binding domains using various sources of plant wall materials and purified xylan. fCBDs also have potential application as affinity tags and could be used to replace affinity tags such as nickel binding histidine repeats and the influenza A virus haemagglutinin (HA) tag for some applications. My studies indicate that the fCBDs on XynA and XynB are attractive candidates because they bound Avicell columns well and the bound proteins could be efficiently eluted under non-denaturing conditions. These preliminary results could be extended by comparing the binding potential for various carbohydrate matrices of these three fCBDs. Future studies could include the development of plasmid vectors for the expression of fusion proteins with fCBDs. These vectors could be useful for the production and affinity purification of proteins.

LITERATURE CITED

Andrews S.R., Charnock S.J., Lakey J.H., Davies G.J., Claeyssens M., Nerinckx W., Underwood M., Sinnott M.L., Warren R.A., Gilbert H.J. 2000. Substrate specificity in glycoside hydrolase family 10. Tyrosine 87 and leucine 314 play a pivotal role in discriminating between glucose and xylose binding in the proximal active site of *Pseudomonas cellulosa* xylanase 10A. J. Biol. Chem. 275:23027-33.

Appel R.D., Bairoch A., Hochstrasser D.F. 1994. A new generation of information retrieval tools for biologists: the example of the ExPASy WWW server. Trends Biochem. Sci. 19:258–260.

Arhin F.F., Shareck F., Kluepfel D., Morosoli R. 1994. Effects of disruption of xylanase-encoding genes on the xylanolytic system of *Streptomyces lividans*. J. Bacteriol. 176:4924-30.

Armand S., Andrews S.R., Charnock S.J., Gilbert H.J. 2001. Influence of the aglycone region of the substrate binding cleft of Pseudomonas xylanase 10A on catalysis. Biochemistry 40:7404-9.

Bajorath J., Stenkamp R. and Aruffo A. 1993. Knowledge-based model building of proteins: concepts and examples. Protein Sci. 2, 1798-1810.

Bajpai P. 2004. Biological bleaching of chemical pulps. Crit. Rev. Biotechnol. 24:1-58.

Berman H.M., Westbrook J., Feng Z., Gilliland G., Bhat T.N., Weissig H., Shindyalov I.N., Bourne P.E. 2000. The protein data bank. Nucleic Acids Res. 28:235–242.

Biely P., Vrsanska M., Tenkanen M., Kluepfel D. 1997. Endo-beta-1,4-xylanase families: differences in catalytic properties. J. Biotechnol. 57:151-66.

Bih F.Y., Wu S.S., Ratnayake C., Walling L.L., Nothnagel E.A., Huang A.H. 1999. The predominant protein on the surface of maize pollen is an endoxylanase synthesized by a *tapetum* mRNA with a long 5' leader. J. Biol. Chem. 274:22884-94.

Black G.W., Rixon J.E., Clarke J.H., Hazlewood G.P., Theodorou M.K., Morris P., Gilbert H.J. 1996. Evidence that linker sequences and cellulose-binding domains enhance the activity of hemicellulases against complex substrates. Biochem. J. 15:515–520.

Blanco A., Diaz P., Zueco J., Parascandola P., Javier Pastor F.I. 1999. A multidomain xylanase from a *Bacillus sp.* with a region homologous to thermostabilizing domains of thermophilic enzymes. Microbiology 145:2163-70.

Cameron M.D., Timofeevski S., Aust S.D. 2000. Enzymology of *Phanerochaete chrysosporium* with respect to the degradation of recalcitrant compounds and xenobiotics. Appl. Microbiol. Biotechnol. 54:751-8.

Carrard G., Linder M. 1999.Widely different off rates of two closely related cellulose-binding domains from *Trichoderma reesei*. Eur. J. Biochem. 262:637-43.

Carrard G., Koivula A., Soderlund H., Beguin P. 2000. Cellulose-binding domains promote hydrolysis of different sites on crystalline cellulose. Proc. Natl. Acad. Sci. USA 97:10342–10347.

Carrez D., Janssens W., Degrave P., van den Hondel C.A., Kinghorn J.R., Fiers W., Contreras R. 1990. Heterologous gene expression by filamentous fungi: secretion of human interleukin-6 by *Aspergillus nidulans*. Gene 94:147-54.

Charnock S.J., Lakey J.H., Virden R., Hughes N., Sinnott M.L., Hazlewood G.P., Pickersgill R., Gilbert H.J. 1997. Key residues in subsite F play a critical role in the activity of *Pseudomonas fluorescens* subspecies cellulosa xylanase A against xylooligosaccharides but not against highly polymeric substrates such as xylan. J. Biol. Chem. 272:2942-51.

Charnock S.J., Spurway T.D., Xie H., Beylot M.H., Virden R., Warren R.A., Hazlewood G.P., Gilbert H.J. 1998. The topology of the substrate binding clefts of glycosyl hydrolase family 10 xylanases are not conserved. J. Biol. Chem. 273:32187-99.

Chothia C. and Lesk A. M.1986. The relation between the divergence of sequence and structure in proteins. EMBO J. 5, 823-826

Christakopoulos P., Katapodis P., Kalogeris E., Kekos D., Macris B.J., Stamatis H., Skaltsa H. Antimicrobial activity of acidic xylo-oligosaccharides produced by family 10 and 11 endoxylanases. Int. J. Biol. Macromol. 2003. 31:171-5.

Clarke J.H., Rixon J.E., Ciruela A., Gilbert H.J., Hazlewood G.P. 1997.Family-10 and family-11 xylanases differ in their capacity to enhance the bleachability of hardwood and softwood paper pulps. Appl. Microbiol. Biotechnol. 48:177-83.

Collins T., Meuwis M.A., Stals I., Claeyssens M., Feller G., Gerday C. 2002. A novel family 8 xylanase, functional and physicochemical characterization. J. Biol. Chem. 277:35133-9.

Coutinho P.M. Henrissat B. 1999. Carbohydrate-Active Enzymes server at URL: http://afmb.cnrs-mrs.fr/CAZY/

Davies G., Henrissat B. 1995. Structures and mechanisms of glycosyl hydrolases. Structure 3:853–859.

Debets A.J.M. and Bos C.J. 1986. Isolation of small protoplasts from *Aspergillus niger*. FGN. 33:24.

De Lemos Esteves F., Ruelle V., Lamotte-Brasseur J., Quinting B., Frere J.M. 2004. Acidophilic adaptation of family 11 endo-{beta}-1,4-xylanases: Modeling and mutational analysis. Protein Sci. 1209-1218.

Derewenda U., Swenson .L, Green R., Wei Y, Morosoli R., Shareck F., Kluepfel D., Derewenda Z.S. 1994. Crystal structure, at 2.6-A resolution, of the *Streptomyces lividans* xylanase A, a member of the F family of beta-1,4-D-glycanases. J. Biol. Chem. 269:20811-4.

Dickinson J.R.and Schweizer M. 1998. Metabolism and Molecular Physiology of *Saccharomyces Cerevisiae.* CRC Press publishing.

Dhawale S.S., Kessler K. 1993. Alternative methods for production and staining of *Phanerochaete chrysosporium* basidiospores. Appl. Environ. Microbiol. 59:1675-7.

Dominguez R., Souchon H., Spinelli S., Dauter Z., Wilson K.S., Chauvaux S., Beguin P., Alzari P.M. 1995. A common protein fold and similar active site in two distinct families of beta-glycanases. Nat. Struct. Biol. 2:569-76.

Ducros V., Charnock S.J., Derewenda U., Derewenda Z.S., Dauter Z., Dupont C., Shareck F., Morosoli R., Kluepfel D., Davies G.J. 2000. Substrate specificity in glycoside hydrolase family 10. Structural and kinetic analysis of the *Streptomyces lividans* xylanase 10A. J. Biol. Chem. 275:23020-6.

Emami K., Nagy T., Fontes C.M., Ferreira L.M., Gilbert H.J. 2002. Evidence for temporal regulation of the two *Pseudomonas cellulosa* xylanases belonging to glycoside hydrolase family 11. J. Bacteriol. 184:4124-33.

Fowler T., Berka R.M., Ward M. 1990. Regulation of the glaA gene of *Aspergillus niger*. Curr. Genet. 18:537-45.

Fushinobu S., Ito K., Konno M., Wakagi T., Matsuzawa H. 1998. Crystallographic and mutational analyses of an extremely acidophilic and acid-stable xylanase: biased distribution of acidic residues and importance of Asp37 for catalysis at low pH. Protein Eng. 1121-8.

Gilkes N.R., Henrissat B., Kilburn D.G., Miller R.C. Jr., Warren R.A. 1991. Domains in microbial beta-1, 4-glycanases: sequence conservation, function, and enzyme families. Microbiol. Rev. 55:303-15.

Glazer A. W., Hiroshi N. 1995. Microbial Biotechnology, Fundamentals of Applied Microbiology W. H. Freeman. New York.

Gordon C.L., Khalaj V., Ram A.F., Archer D.B., Brookman J.L., Trinci A.P., Jeenes D.J., Doonan J.H., Wells B., Punt P.J., van den Hondel C.A., Robson G.D. 2000. Glucoamylase::green fluorescent protein fusions to monitor protein secretion in *Aspergillus niger*. Microbiology 146:415-26.

Guex N., Peitsch M.C. 1997. SWISS-MODEL and the Swiss-PdbViewer: an environment for comparative protein modelling. Electrophoresis 18:2714–2723.

Harris G.W., Jenkins J.A., Connerton I., Cummings N., Lo Leggio L., Scott M., Hazlewood G.P., Laurie J.I., Gilbert H.J., Pickersgill R.W. 1994.Structure of the catalytic

core of the family F xylanase from *Pseudomonas fluorescens* and identification of the xylopentaose-binding sites. Structure 2:1107-16.

Hanahan D. 1983. Studies on transformation of *Escherichia coli* with plasmids. J. Mol. Biol. 166:557-80.

Harrison R. W., Chatterjee D. and Weber I. T. 1995. Analysis of six protein structures predicted by comparative modeling techniques. Proteins Struct. Func. Genet. 23, 463-471.

Hata Y., Kitamoto K., Gomi K., Kumagai C., Tamura G. 1992. Functional elements of the promoter region of the *Aspergillus oryzae* glaA gene encoding glucoamylase. Curr. Genet. 22:85-91.

Henikoff S. and Henikoff J. G. 1992. Amino acid substitution matrices from protein blocks. Proc. Natl. Acad. Sci. USA 89:10915-10919.

Henrissat B. 1991. A classification of glycosyl hydrolases based on amino acid sequence similarities. Biochem. J. 280: 309-316.

Henrissat B., Davies G. 1997. Structural and sequence-based classification of glycoside hydrolases. Curr. Opin. Struct. Biol. 7:637-44.

Henrissat B., Davies G.J. 2000. Glycoside hydrolases and glycosyltransferases. Families, modules, and implications for genomics. Plant. Physiol. 124:1515-9.

Hrmova M., Petrakova E., Biely P. 1991. Induction of cellulose- and xylan-degrading enzyme systems in *Aspergillus terreus* by homo- and heterodisaccharides composed of glucose and xylose. J. Gen. Microbiol. 137:541-7.

Jacobs A., Larsson P.T., Dahlman O. 2001. Distribution of uronic acids in xylans from various species of soft- and hardwood as determined by MALDI mass spectrometry. Biomacromolecules 2:979-90.

Jeenes D.J., Marczinke B., MacKenzie D.A., Archer D.B. 1993. A truncated glucoamylase gene fusion for heterologous protein secretion from *Aspergillus niger*. FEMS Microbiol. Lett. 107:267-71.

Jeenes D.J., Mackenzie D.A., Archer D.B. 1994. Transcriptional and post-transcriptional events affect the production of secreted hen egg white lysozyme by *Aspergillus niger*. Transgenic. Res. 3:297-303.

Joshi M.D., Sidhu G., Pot I., Brayer G.D., Withers S.G., McIntosh LP. 2000. Hydrogen bonding and catalysis: a novel explanation for how a single amino acid substitution can change the pH optimum of a glycosidase. J. Mol. Biol. 299:255-79.

Käfer E. 1977. Meiotic and mitotic recombination in *Aspergillus* and its chromosomal aberrations. Adv. Genet. 19:33–131.

Kersten P.J., Witek C., vanden Wymelenberg A., Cullen D.1995. *Phanerochaete chrysosporium* glyoxal oxidase is encoded by two allelic variants: structure, genomic organization, and heterologous expression of glx1 and glx2. J. Bacteriol. 177:6106-10.

Koch, Peter. 1985. Utilization of Hardwoods Growing on Southern Pine Sites. USDA Forest Service publishing.

Kosugi A., Murashima K., Doi R.H. 2002. Xylanase and acetyl xylan esterase activities of XynA, a key subunit of the *Clostridium cellulovorans* cellulosome for xylan degradation. Appl. Environ. Microbiol. 68:6399-402.

Kratky Z., Biely P. 1980. Inducible beta-xyloside permease as a constituent of the xylan-degrading enzyme system of the yeast *Cryptococcus albidus*. Eur. J. Biochem. 112:367-73.

Kraulis J., Clore G.M., Nilges M., Jones T.A., Pettersson G., Knowles J., Gronenborn A.M. 1989. Determination of the three-dimensional solution structure of the C-terminal domain of cellobiohydrolase I from *Trichoderma reesei*. A study using nuclear magnetic resonance and hybrid distance geometry-dynamical simulated annealing. Biochemistry 28:7241-57.

Krengel U., Dijkstra B.W. 1996. Three-dimensional structure of Endo-1,4-beta-xylanase I from *Aspergillus niger*: molecular basis for its low pH optimum. J. Mol. Biol. 263:70-8.

Kulkarni N., Shendye A., Rao M. 1999. Molecular and biotechnological aspects of xylanases. FEMS Microbiol. Rev. 23:411-56.

Lappalainen A., Siika-Aho M., Kalkkinen N., Fagerstrom R., Tenkanen M. 2000. Endoxylanase II from *Trichoderma reesei* has several isoforms with different isoelectric points. Biotechnol. Appl. Biochem. 31:61-8.

Leggio L.L., Jenkins J., Harris G.W., Pickersgill R.W. 2000. X-ray crystallographic study of xylopentaose binding to *Pseudomonas fluorescens* xylanase A. Proteins 41:362-73.

Li B., Nagalla S.R., Renganathan V. 1997. Cellobiose dehydrogenase from *Phanerochaete chrysosporium* is encoded by two allelic variants. Appl. Environ. Microbiol. 63:796-9.

Linder M., Mattinen M.L., Kontteli M., Lindeberg G., Stahlberg J., Drakenberg T., Reinikainen T., Pettersson G., Annila A. 1995. Identification of functionally important amino acids in the cellulose-binding domain of *Trichoderma reesei* cellobiohydrolase I. Protein Sci. 6:1056-64.

Linder M., Lindeberg G., Reinikainen T., Teeri T.T., Pettersson G. 1995. The difference in affinity between two fungal cellulose-binding domains is dominated by a single amino acid substitution. FEBS Lett. 372:96-8.

Linder M., Nevanen T., Teeri T.T. 1999. Design of a pH-dependent cellulose-binding domain. FEBS Lett. 19;447:13-6.

Lubomir K., Peter B. 1998. Disaccharides permeases: constituents of xylanolytic and mannanolytic systems of *Aureobasidium pullulans*. Biochim. Biophys. Acta. 1425:560-6.

Mattinen M.L., Linder M., Teleman A., Annila A. 1997. Interaction between cellohexaose and cellulose binding domains from *Trichoderma reesei* cellulases.
FEBS Lett. 5;407:291-6.

Mattinen M.L., Linder M., Drakenberg T., Annila A. 1998. Solution structure of the cellulose-binding domain of endoglucanase I from *Trichoderma reesei* and its interaction with cello-oligosaccharides. Eur. J. Biochem. 256:279-86.

McLauchlan W.R., Garcia-Conesa M.T., Williamson G., Roza M., Ravestein P., Maat J. 1999. A novel class of protein from wheat which inhibits xylanases. Biochem. J. 338:441-6.

Moreau A., Shareck F., Kluepfel D., Morosoli R. 1994. Alteration of the cleavage mode and of the transglycosylation reactions of the xylanase A of *Streptomyces lividans* 1326 by site-directed mutagenesis of the Asn173 residue. Eur. J. Biochem. 219:261-6.

Nakamura S, Wakabayashi K, Nakai R, Aono R, Horikoshi K. 1993. Purification and some properties of an alkaline xylanase from alkaliphilic *Bacillus* sp. strain 41M-1.
Appl. Environ. Microbiol. 59:2311-6.

Nielsen H., Engelbrecht J., Brunak S., Heijne G. von.1997. Identification of prokaryotic and eukaryotic signal peptides and prediction of their cleavage sites. Protein. Eng. 10:1–6.

Nunberg J.H., Meade J.H., Cole G., Lawyer F.C., McCabe P., Schweickart V., Tal R., Wittman V.P., Flatgaard J.E., Innis M.A. 1984. Molecular cloning and characterization of the glucoamylase gene of *Aspergillus awamori*. Mol. Cell. Biol. 4:2306-15.

Palonen H., Tenkanen M., Linder M. 1999. Dynamic interaction of *Trichoderma reesei* cellobiohydrolases Cel6A and Cel7A and cellulose at equilibrium and during hydrolysis.
Appl. Environ. Microbiol. 65:5229-33.

Peitsch M.C. 1995. Protein modeling by e-mail. Bio/Technology. 13:658–666.

Pell G., Taylor E.J., Gloster T.M., Turkenburg J.P., Fontes C.M., Ferreira L.M., Nagy T., Clark S.J., Davies G.J., Gilbert H.J. The mechanisms by which family 10 glycoside hydrolases bind decorated substrates. 2004. J. Biol. Chem. 279:9597-605.

Piontek K., Smith A.T., Blodig W. 2001. Lignin peroxidase structure and function.
Biochem. Soc. Trans. 29:111-6.

Punt P.J., van Biezen N., Conesa A., Albers A., Mangnus J., van den Hondel C. 2002. Filamentous fungi as cell factories for heterologous protein production.
Trends Biotechnol. 20:200-6.

Purves W.K.1998. Life, the science of biology. Sunderland, Mass. Publishing Salt Lake City, Utah.

Reinikainen T., Ruohonen L., Nevanen T., Laaksonen L., Kraulis P., Jones T.A., Knowles J.K., Teeri T.T. 1992. Investigation of the function of mutated cellulose-binding domains of *Trichoderma reesei* cellobiohydrolase I. Proteins 14:475–482.

Rose K.C. 2003. The plant cell wall. Annual Plant reviews, Vol 8. CRC press. Blackwell publishing. Oxford

Santerre Henriksen A.L., Even S., Muller C., Punt P.J., van den Hondel C.A., Nielsen J. 1999. Study of the glucoamylase promoter in *Aspergillus niger* using green fluorescent protein. Microbiology 145:729-34.

Sapag A., Wouters J., Lambert C., de Ioannes P., Eyzaguirre J., Depiereux E. 2002. The endoxylanases from family 11: computer analysis of protein sequences reveals important structural and phylogenetic relationships. J. Biotechnol. 95:109-31.

Schmidt A., Schlacher A., Steiner W., Schwab H., Kratky C. 1998. Structure of the xylanase from *Penicillium simplicissimum*. Protein Sci. 7:2081-8.

Schwede T., Kopp J., Guex N., Peitsch M.C. 2003. SWISS-MODEL: an automated protein homology-modeling server. Nucleic. Acids Res. 31:3381–3385.

Sengupta S., Jana M.L., Sengupta D., Naskar A.K. 2000. A note on the estimation of microbial glycosidase activities by dinitrosalicylic acid reagent. Appl. Microbiol. Biotechnol. 53:732–735.

Srisodsuk M., Reinikainen T., Penttila M., Teeri T.T. 1993. Role of the interdomain linker peptide of *Trichoderma reesei* cellobiohydrolase I in its interaction with crystalline cellulose. J. Biol. Chem. 268:20756-61.

Stewart P., Gaskell J., Cullen D. 2000. A homokaryotic derivative of a *Phanerochaete chrysosporium* strain and its use in genomic analysis of repetitive elements. Appl. Environ. Microbiol. 66:1629-33.

Storms R., Zheng Y., Li H, Sillaots S., Martinez-Perez A., Tsang A. 2005. Plasmid vectors for protein production, gene expression and molecular manipulations in *Aspergillus niger*. Plasmid 53:191-204.

Tahir T.A., Berrin J.G., Flatman R., Roussel A., Roepstorff P., Williamson G., Juge N. 2002. Specific characterization of substrate and inhibitor binding sites of a glycosyl hydrolase family 11 xylanase from *Aspergillus niger*. J. Biol. Chem. 277:44035-43. Epub 2002 Aug 30.

Teleman A., Tenkanen M., Jacobs A., Dahlman O. 2002. Characterization of O-acetyl-(4-O-methylglucurono)xylan isolated from birch and beech. Carbohydr. Res. 337:373-7.

Thompson, W., and P. Broda. 1987. Mating behaviour in an isolate of *Phanerochaete chrysosporium*. Trans. Br. Mycol. Soc. 89:285-294.

Tomme P., Van Tilbeurgh H., Pettersson G., Van Damme J., Vandekerckhove J., Knowles J., Teeri T., Claeyssens M. 1988. Studies of the cellulolytic system of *Trichoderma reesei* QM 9414. Analysis of domain function in two cellobiohydrolases by limited proteolysis. Eur. J. Biochem.170:575-81.

Torronen A., Harkki A., Rouvinen J. 1994.Three-dimensional structure of endo-1,4-beta-xylanase II from *Trichoderma reesei*: two conformational states in the active site. EMBO J. 13:2493-501.

Torronen A., Rouvinen J. 1995. Structural comparison of two major endo-1,4-xylanases from *Trichoderma reesei*. Biochemistry 34:847-56.

Turunen O., Vuorio M., Fenel F, Leisola M. 2002. Engineering of multiple arginines into the Ser/Thr surface of *Trichoderma reesei* endo-1,4-beta-xylanase II increases the thermotolerance and shifts the pH optimum towards alkaline pH. Protein Eng. 15:141-5.

Vardakou M., Katapodis P., Samiotaki M., Kekos D., Panayotou G., Christakopoulos P. 2003. Mode of action of family 10 and 11 endoxylanases on water-unextractable arabinoxylan. Int. J. Biol. Macromol. 33:129-34.

Verdoes J.C., Punt P.J., Schrickx J.M., van Verseveld H.W., Stouthamer A.H., van den Hondel C.A. 1993. Glucoamylase overexpression in *Aspergillus niger*: molecular genetic analysis of strains containing multiple copies of the glaA gene. Transgenic. Res. 2:84-92.

Vrsanska M., Hirsch J., Kovac P., Biely P. 1990. Hydrolysis of (1----3)- and (1----2)-beta-D-xylosidic linkages by an endo-(1----4)-beta-D-xylanase of *Cryptococcus albidus*. Carbohydr. Res. 206:251-6.

Wakarchuk W.W., Campbell R.L., Sung W.L., Davoodi J., Yaguchi M. 1994. Mutational and crystallographic analyses of the active site residues of the *Bacillus circulans* xylanase. Protein Sci.:467-75.

White A., Withers S.G., Gilkes N.R., Rose D.R. 1994. Crystal structure of the catalytic domain of the beta-1,4-glycanase cex from *Cellulomonas fimi*. Biochemistry 33:12546-52.

Withers J.M., Swift R.J., Wiebe M.G., Robson G.D., Punt P.J., van den Hondel C.A., Trinci A.P. 1998. Optimization and stability of glucoamylase production by recombinant strains of *Aspergillus niger* in chemostat culture. Biotechnol. Bioeng. 59:407-18.

Young R.A. and Akhtar M. 1997. Environmentally Friendly Technologies for the Pulp and Paper Industry. John Wiley and Sons Ltd Publishing.

Zechel D.L., Withers S.G. 2001. Dissection of nucleophilic and acid-base catalysis in glycosidases. Curr. Opin. Chem. Biol. 5:643-9.

Zito R. 2003. The molecular characterization of the glucoamylase and pyruvate kinase genes of *Aspergillus niger.* Master thesis. Concordia University